

Supporting Information for

Evaluation of 3-ethyl-3-(phenylpiperazinylbutyl)oxindoles as PET Ligands for the Serotonin 5-HT₇ Receptor – Synthesis, Pharmacology, Radiolabeling and in vivo Brain Imaging in Pigs

Matthias M. Herth,^{§,†} Valdemar L. Andersen,^{§,†} Hanne D. Hansen,[§] Nikolas Stroth,[‡] Balázs Volk,[‡] Anders Ettrup,[§] Szabolcs Lehel,[#] Per Svenningsson,[‡] Gitte M. Knudsen,[§] Jesper L. Kristensen.^{§,†}

§Center for Integrated Molecular Brain Imaging, Rigshospitalet and University of Copenhagen, Blegdamsvej 9, DK-2100 Copenhagen, Denmark. †Department of Drug Design and Pharmacology, Faculty of Health and Medical Sciences, University of Copenhagen, Universitetsparken 2, DK-2100 Copenhagen, Denmark. ‡Center for Molecular Medicine, Department of Neurology and Clinical Neuroscience, Karolinska Institute and Karolinska University Hospital, 17176 Stockholm, Sweden ‡Egis Pharmaceuticals Plc., P.O. Box 100, H-1475 Budapest, Hungary. #PET and Cyclotron Unit, Rigshospitalet, Blegdamsvej 9, DK-2100 Copenhagen, Denmark.

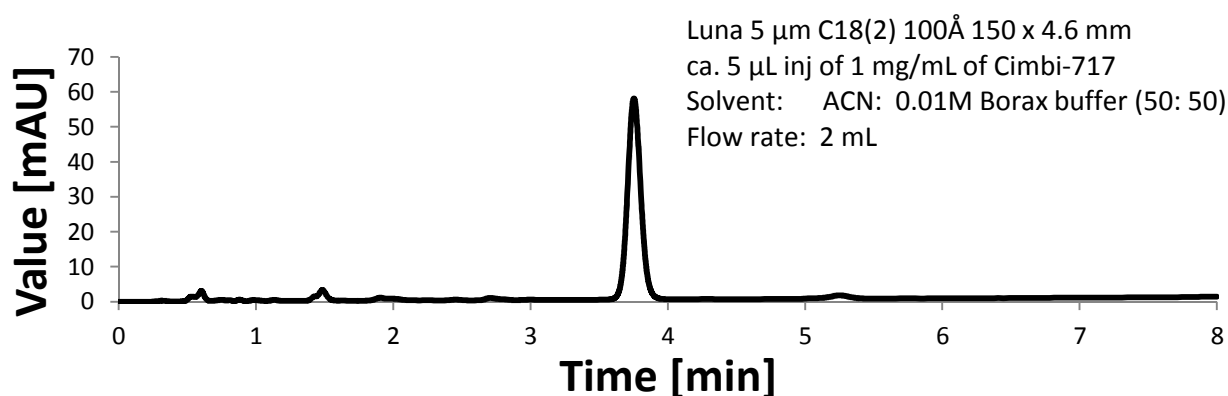
Table of contents

1. Chiral resolution of 3-unsubstituted 3-phenylpiperazinyl-butylloxindoles	S1
2. General	S2
3. Structure-activity studies of 3-alkyl-3-(phenylpiperazinylbutyl)oxindoles	S2
4. Organic syntheses	S6
5. Chiral resolution and stability test of 3 and 4 .	S11
6. PDSP Screening	S14
7. Receptor distribution of co-localized targets	S15
8. Selectivity/B _{max} ratio for 5-HT ₇	S15
9. In vitro characterization	S16
10. Determination of lipophilicity	S17
11. Preparative radio-HPLC chromatogram of [¹¹ C]- 4 ([¹¹ C]-Cimbi-775)	S19
12. Preparative radio-HPLC chromatogram of [¹¹ C]- 3 ([¹¹ C]-Cimbi-772)	S20
13. Analytical HPLC chromatogram of [¹¹ C]- 3 and [¹¹ C]- 4 .	S21
14. Determination of radiochemical purity and specific radioactivity	S22
15. In vitro autoradiography	S22
16. Animal procedures	S24
17. Quantification of PET data	S24
18. References	S25
19.	S26

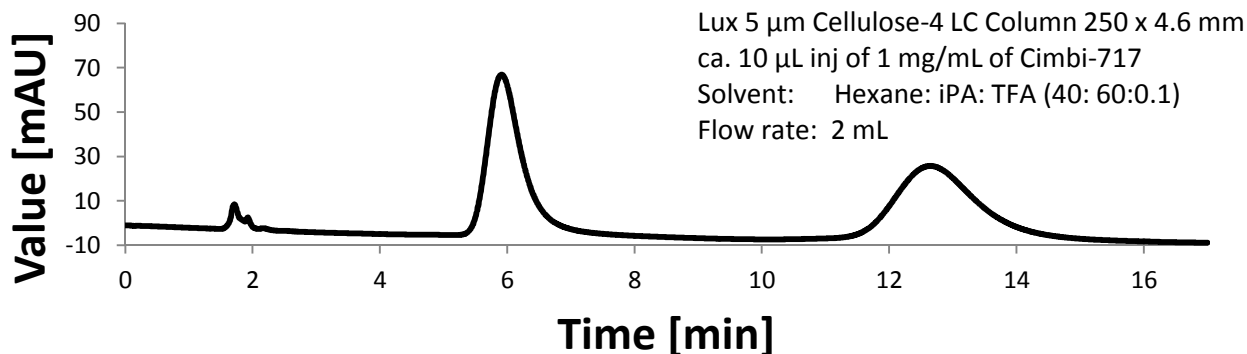
1. Chiral resolution of 3-unsubstituted 3-(phenylpiperazinylbutyl)oxindoles

1 (Cimbi-712) and **2** (Cimbi-717) were separated using chiral HPLC. Figure a) shows the purity of Cimbi-717, whereas b) the chiral resolution of Cimbi-717, while c) displays the chiral resolution of Cimbi-712. Unfortunately, reinjection of both separated fractions showed epimerisation after 5 minutes. Complete conversion was observed within 30 minutes.

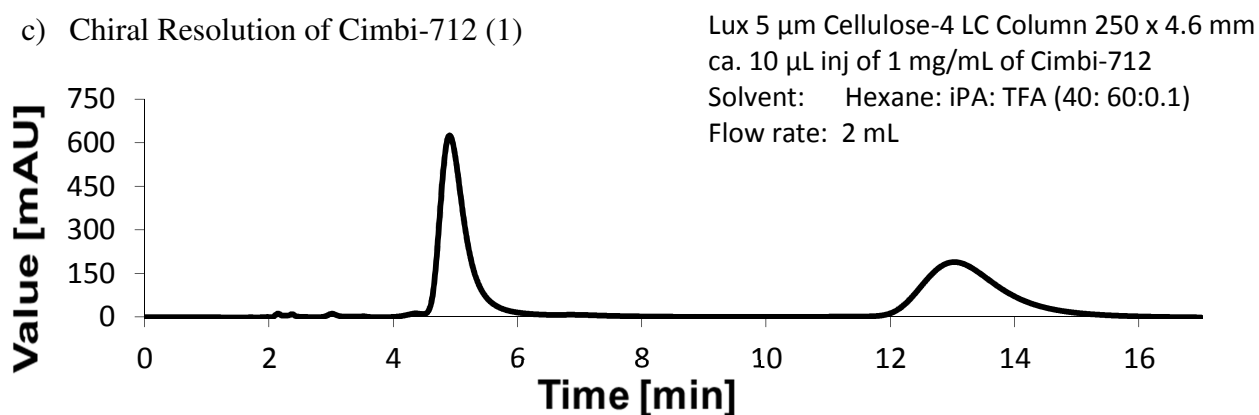
a) RP-HPLC of Cimbi-717 (2)



b) Chiral Resolution of Cimbi-717 (2)



c) Chiral Resolution of Cimbi-712 (1)

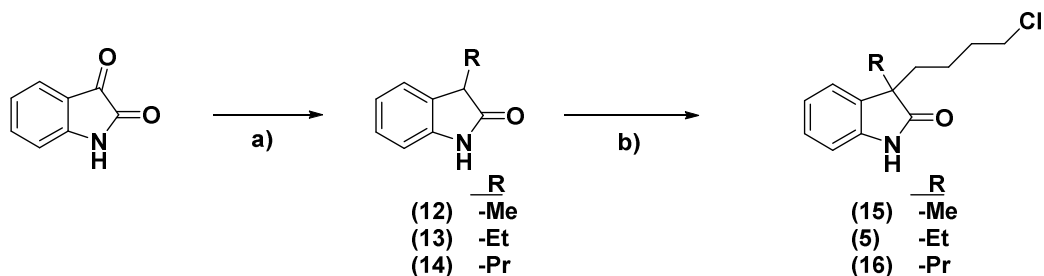


2. General

Chemicals were purchased from Acros, Fluka, Sigma, Tocris, ABX or Merck. Unless otherwise stated, all chemicals were used without further purification. Flash chromatography was performed on silica gel 60 (35-70 μm). Thin layer chromatography (TLC) was performed using plates from Merck (silica gel 60 F₂₅₄ and aluminium oxide 60 F₂₅₄). ¹H-NMR and ¹³C-NMR spectra were recorded using a Bruker AC 300 spectrometer or a Bruker AC 400 spectrometer. Chemical shifts are quoted as δ values (ppm) downfield from tetramethylsilane (TMS) internal standard. Infrared spectroscopy was performed on a Perkin Elmer FT-IR Spektrometer (Spectrum One). Melting points were determined on a Stanford Research Systems Optimelt system. For solid phase extraction (SPE), Sep-Pak®-C18-cartridges (Waters, USA) were used. GC-MS measurements were performed on a Shimadzu apparatus (GCMS-QP 5050). LC-MS tests were performed on 6410 Triple Quad LC/MS instrument. Field desorption mass spectra (FD-MS) were recorded using a Finnigan MAT90 spectrometer and electrospray ionization mass spectrometry (ESI-MS) were performed on a ThermoQuest Navigator-Instrument. High resolution mass spectra (HRMS) were recorded on a Q-TOF Premier (Waters, USA) and Maxis Impact (BrukerDaltonics, Germany) spectrometer. Analytical and preparative high performance liquid chromatography (HPLC) were performed on a Dionex system consisting of a P680A pump, a UVD 170U detector and a Scansys radiodetector. Lipophilicities were determined using a Dionex Ultimate 3000 HPLC equipped with a degasser, an autosampler, a column-oven and a UV-detector. Chiral resolution was performed on a Lux 5 μm Cellulose-4 LC Column 250 x 4.6 mm. PET scanning was performed with a high-resolution research tomography scanner (HRRT, Siemens AG). [¹¹C]Methane was produced via the ¹⁴N(p, α)¹¹C reaction by bombardment of an [¹⁴N]N₂ containing 10% H₂ target with a 17 MeV proton beam in a Scanditronix MC32NI cyclotron. Full spectral data of previously published compounds can be found in the indicated references.

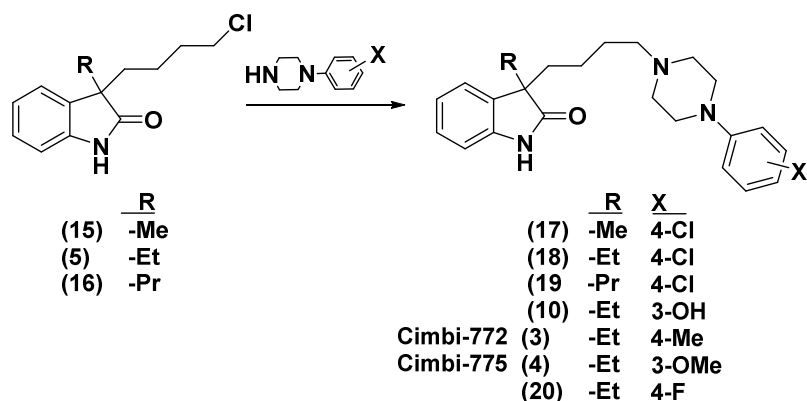
3. Structure-activity-studies of 3-alkyl-3-(phenylpiperazinylbutyl)oxindoles

A convenient organic synthetic route to 3-alkyl-3-(ω -chloroalkyl)oxindoles has been described by Volk et al. [1]. Briefly, isatins were reductively alkylated with alcohols in the presence of Raney nickel under hydrogen pressure. The resulting 3-alkyloxindoles were further C-3 alkylated using 2 equivalents *n*-BuLi and 1,4-bromochlorobutane (Scheme 1). The resulted intermediates obtained were finally linked to 1-(4-chlorophenyl)piperazine by applying neat reaction conditions (Scheme S2).



Scheme S1: General procedure for the preparation of 3-alkyl-3-(4-chlorobutyl)oxindoles: a) ROH, Ra-Ni, 15 bar H₂, 180 °C, 3-4 h, 85-95% b) n-BuLi, Br-(CH₂)₄-Cl, THF, from -78 °C to RT, 4h, > 80%

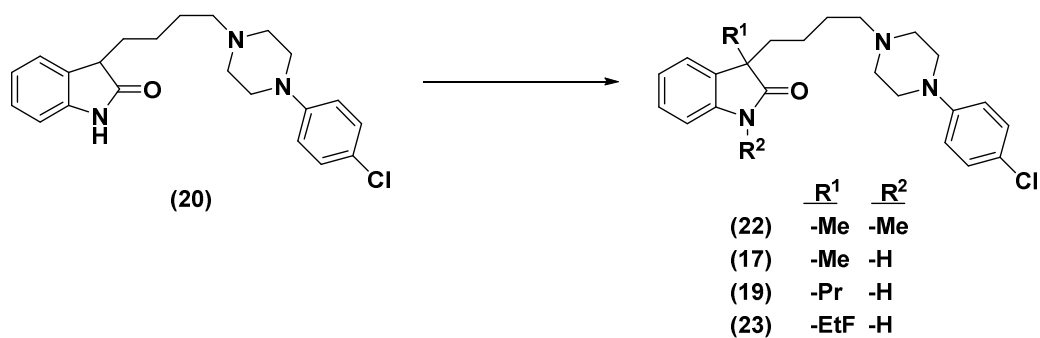
In general, fewer products were observed using these chloro-intermediates compared to previously applied mesylates, even at higher reaction temperature [2]. Furthermore, in contrast to the mesylated derivative, the halogenated compound did not decompose at room temperature.



Scheme S2: Synthesis of 3-alkyloxindole derivatives: Na₂CO₃, 180 °C, 1h, 73-85%

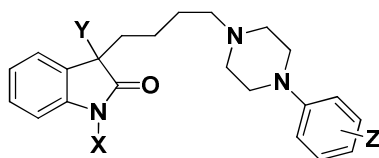
The second approach aiming at a C-3 alkylation at a later stage, only resulted in limited success (Scheme S3). Use of methyl iodide lead to dimethylation (in addition to the C-3-position, the N-1 position was also alkylated), whereas the alkylation with propyl iodide failed. Alkylation with 1,2-bromofluoroethane resulted in the desired product, however only in 24%. Therefore, alkylation earlier in the synthesis sequence is preferable.

In a next evaluation step, the affinity towards the 5-HT₇ receptor binding site was determined. Alkylation at the C-3 position of the oxindole did not alter the affinity towards the 5-HT₇ receptor significantly. Low nanomolar K_i values below 10 nM were detected for all reference compounds and consequent labeling should thus enable 5-HT₇ PET imaging (Table S1). Only one exception could be detected. Dialkylation leading to compound (22) reduced the affinity by a factor of 5-8. This is in line with previously reported data [1].



Scheme S3: C-3 alkylation of oxindole derivatives with alkylhalides: n-BuLi, RX, THF, from -78 °C to RT, 12 h, 0-55%

Table S1: Human recombinant 5-HT₇ affinity: The influence of the C-3 position of the oxindole



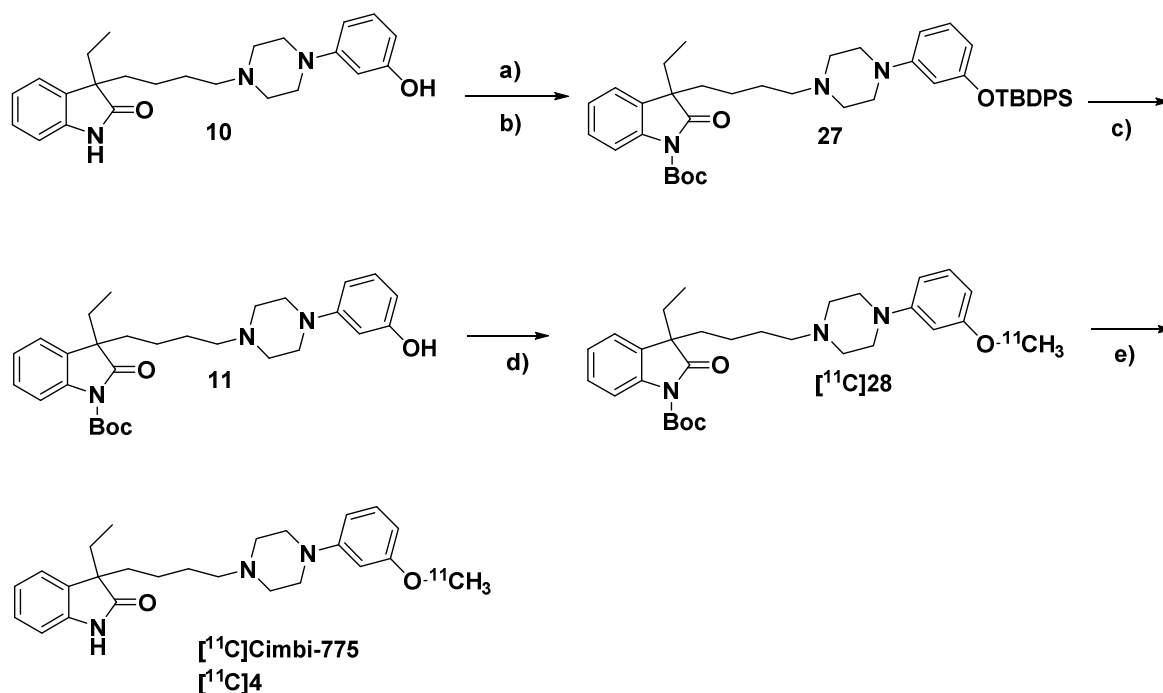
compound	Z	X	Y	5-HT ₇ ^a K _i (nM)	LogD _{7.4}
24	4-Cl	-H	-H	7.0	4.56
17	4-Cl	-H	-Me	1.2	4.98
18	4-Cl	-H	-Et	0.7	5.76
23	4-Cl	-H	-EtF	1.4	5.72
19	4-Cl	-H	-Pr	3.5	5.92
22	4-Cl	-Me	-Me	16	> 7
Cimbi-717 (2)	3-OMe	-H	-H	7.5	4.73
Cimbi-775 (4)	3-OMe	-H	-Et	7.8	5.75
(+)-4	3-OMe	-H	-Et	11	5.75
(-)-4	3-OMe	-H	-Et	56	5.75
25	4-F	-H	-H	1.1	4.65
20	4-F	-H	-Et	0.5	5.72
26	3-OH	-H	-H	27.5	3.40
10	3-OH	-H	-Et	8.9	4.40
Cimbi-712 (1)	4-Me	H	-H	4.1	5.19
Cimbi-772 (3)	4-Me	H	-Et	6.5	6.17
(+)-3	4-Me	H	-Et	5.6	6.17
(-)-3	4-Me	H	-Et	82	6.17

Affinities were determined by PDSP

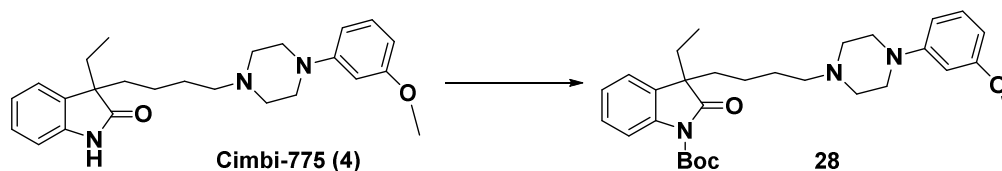
4. Organic syntheses

Compounds **12**, **13**, **14**, **5**, **18**, **20**, **24**, **25**, **26**, **6**, Cimbi-712 (**1**), Cimbi-717 (**2**) and Cimbi-775 (**4**) were synthesized as previously published [1-4].

General synthesis strategies:



Scheme S4: Synthesis of the precursor and $[^{11}\text{C}]$ Cimbi-775: a) TBDPSCl, NaH, DMF, 110 °C, 12 h; b) Boc_2O , NaHDMs, THF, -5 °C, 30 min; c) NH_4F , MeOH, 70 °C, 30 min; d) $[^{11}\text{C}]\text{CH}_3\text{I}$, 2M NaOH, DMF, 140 °C, 5 min; e) TFA/ CH_2Cl_2 (1:1), 80 °C, 5 min.



Scheme S5: Synthesis of **u**: Boc_2O , NaHDMs, THF, -5 °C, 30 min

General procedure for the preparation of 3-alkyl-3-(4--chloroalkyl)oxindoles.

To a mixture of *n*-BuLi in hexane (2.5 M, 20 mL, 0.05 mol) and THF (20 mL), the solution of the appropriate 3-alkyloxindole (0.02 mol) in THF (25 mL) was added dropwise at $-78\text{ }^{\circ}\text{C}$, under argon atmosphere. Then the 1-bromo-4-chlorobutane (3.38 g, 0.02 mol) was added dropwise, and the reaction mixture was allowed to warm to room temperature. The stirring was continued for 3 additional hours, the mixture was quenched with ethanol (20 mL), and the solvents were evaporated. The residue was dissolved in ethyl acetate and extracted with water. The organic layer was dried over Na_2SO_4 and evaporated. The oily residue crystallized upon trituration with hexane (20 mL). The white solid was filtered, washed with hexane, and dried. The products were used without further purification.

3-(4-Chlorobutyl)-3-methyl-1,3-dihydro-2*H*-indol-2-one (**15**)

n-BuLi in hexane (2.5 M, 20 mL, 0.05 mol), 3-methyloxindole (2.95 g, 0.02 mol) and 1-bromo-4-chlorobutane (3.38 g, 0.02 mol), yielded in (**15**) (3.88 g, 16.4 mmol, 82%) as a white solid. Mp $94\text{--}95\text{ }^{\circ}\text{C}$. ^1H NMR (CDCl_3 , 300 MHz): δ 8.74 (1H, bs), 7.24–7.13 (2H, m), 7.06–7.01 (1H, m), 6.92 (1H, d, $J = 7.5\text{ MHz}$), 3.40 (2H, t, $J = 6.0\text{ Hz}$), 1.98–1.88 (1H, m), 1.82–1.61 (3H, m), 1.39 (3H, s), 1.30–1.17 (1H, m), 1.14–0.99 (1H, m). ^{13}C NMR (CDCl_3 , 75 MHz): δ 183.3, 140.5, 134.4, 127.9, 122.9, 122.7, 110.0, 49.0, 44.7, 37.7, 32.7, 24.0, 22.1. LCMS (ESI) RT: 3.68 min, m/z : 238.1 $[\text{M}+\text{H}]^+$ at 210 and 254 nm. R_f : 0.46 (EtOAc/heptane 1:1).

3-(4-Chlorobutyl)-3-propyl-1,3-dihydro-2*H*-indol-2-one (**16**)

n-BuLi in hexane (2.5 M, 20 mL, 0.05 mol), 3-propyloxindole (3.50 g, 0.02 mol) and 1-bromo-4-chlorobutane (3.38 g, 0.02 mol) yielded in (**16**) (3.92 g, 14.8 mmol, 74%) as a white solid. Mp $97\text{--}98\text{ }^{\circ}\text{C}$. ^1H NMR (CDCl_3 , 300 MHz): δ 8.69 (1H, bs), 7.25–7.16 (1H, m), 7.12–7.10 (1H, m), 7.06–7.01 (1H, m), 6.91 (1H, d, $J = 7.5\text{ Hz}$), 3.38 (2H, t, $J = 6.0\text{ Hz}$), 1.95–1.57 (6H, m), 1.28–1.00 (3H, m), 0.94–0.83 (1H, m), 0.78 (3H, t, $J = 9.0\text{ Hz}$). ^{13}C NMR (CDCl_3 , 75 MHz): δ 182.8, 141.2, 132.8, 127.8, 123.1, 122.6, 109.8, 53.7, 44.6, 40.4, 37.3, 32.8, 21.8, 17.6, 14.3. LCMS (ESI) RT: 4.17 min, m/z : 266.1 $[\text{M}+\text{H}]^+$ at 210 and 254 nm. R_f : 0.62 (EtOAc/heptane 1:1).

General Procedure for the coupling of 3-(4-chlorobutyl)-3-alkyloxindoles with 4-piperazines

The secondary amine (12 mmol) was heated to 180 °C under slow stirring. Then 3-(4-chlorobutyl)-3-alkyloxindole (12 mmol) and sodium carbonate (1.36 g, 12 mmol) were added. After 1 h reaction time, the brown melt was cooled to ambient temperature. Ethyl acetate and water were added and the layers were separated. The organic layer was dried over MgSO₄ and evaporated. The residual oil or solid was purified by column chromatography with the indicated eluent.

3-{4-[4-(4-Chlorophenyl)piperazin-1-yl]butyl}-3-methyl-1,3-dihydro-2H-indol-2-one (**17**)

1-(4-Chlorophenyl)-piperazine (0.486 g, 2.48 mmol), sodium carbonate (0.26 g, 2.48 mmol) and 3-(4-chlorobutyl)-3-methyloxindole (0.26 g, 2.48 mmol) yielded in (**17**) (0.71 g, 1.8 mmol, 73%) as a white solid. Compound (**17**) was purified by chromatography using EtOAc as the eluent. Mp 182–183 °C. ¹H NMR (CDCl₃, 300 MHz): δ 8.41 (1H, bs), 7.21–7.12 (4H, m), 7.05–7.00 (1H, m), 6.89 (1H, d, J = 7.5 Hz), 6.78 (2H, d, J = 9.0 Hz), 3.09 (4H, t, J = 6.0 Mz), 2.49 (4H, t, J = 6.0 Mz), 2.24 (2H, t, J = 9.0 Hz), 1.99–1.89 (1H, m), 1.82–1.72 (1H, m), 1.51–1.36 (2H, m), 1.38 (3H, s), 1.20–1.05 (1H, m), 0.99–0.84 (1H, m). ¹³C NMR (CDCl₃, 75 MHz): δ 183.28, 150.03, 140.56, 134.63, 129.06, 127.82, 124.58, 123.03, 122.62, 117.31, 109.86, 58.34, 53.15, 49.20, 49.09, 38.44, 27.01, 24.13, 22.67. LCMS (ESI) RT: 2.41 min, m/z: 398.1 [M+H]⁺ at 210 and 254 nm; R_f: 0.2 (EtOAc). HRMS (ESI) [MH⁺] calcd. for C₂₃H₂₉ClN₃O 398.1999, found 398.2000.

3-{4-[4-(4-Chlorophenyl)piperazin-1-yl]butyl}-3-propyl-1,3-dihydro-2H-indol-2-one (**19**)

1-(4-Chlorophenyl)-piperazine (0.37 g, 1.89 mmol), sodium carbonate (0.2 g, 1.9 mmol) and 3-(4-chlorobutyl)-3-propyloxindole (0.50 g, 1.89 mmol) yielded in (**i**) (0.68 g, 1.60 mmol, 85%) as a white solid. Compound (**19**) was purified by chromatography using EtOAc/heptane 3:1 as the eluent. Mp 129–130 °C. ¹H NMR (CDCl₃, 300 MHz): δ 8.41 (1H, bs), 7.20–7.09 (4H, m), 7.05–7.00 (1H, m), 6.87 (1H, d, J = 7.5 Hz), 6.78 (2H, d, J = 9.0 Hz), 3.09 (4H, t, J = 6.0 Hz), 2.49 (4H, t, J = 6.0 Hz), 2.23 (2H, t, J = 9.0 Hz), 1.97–1.67 (4H, m), 1.47–1.32 (2H, m), 1.16–1.05 (2H, m), 0.96–0.85 (2H, m), 0.78 (3H, t, J = 6.0 Hz). ¹³C NMR (CDCl₃, 75 MHz): δ 183.0, 149.99, 141.41, 133.11, 129.05, 127.73, 124.59, 123.15, 122.51, 117.32, 109.78, 58.31, 53.93, 53.10, 49.15, 40.56, 38.04, 27.01, 22.31, 17.69, 14.43. LCMS (ESI) RT: 2.29 min, m/z: 426.1 [M+H]⁺ at 210 and 254 nm. R_f: 0.3 (EtOAc/heptane 3:1). HRMS (ESI) [MH⁺] calcd. for C₂₅H₃₃ClN₃O 426.2313, found 426.2320.

3-Ethyl-3-{4-[4-(3-hydroxyphenyl)piperazin-1-yl]butyl}-1,3-dihydro-2H-indol-2-one (10).

1-(3-Hydroxyphenyl)piperazine (0.33 g, 1.88 mmol), sodium carbonate (0.2 g, 1.88 mmol) and 3-(4-chlorobutyl)-3-ethyloxindole (0.50 g, 1.88 mmol) yielded in (**j**) (0.49 g, 1.26 mmol, 67%) as a white solid. Compound (**j**) was purified by chromatography using EtOAc as the eluent. Mp 224–225 °C. ¹H NMR (DMSO-*d*₆, 400 MHz): δ 10.99 (1H, bs), 10.41 (1H, s), 7.23–7.16 (2H, m), 7.04–6.98 (2H, m), 6.86 (1H, d, *J* = 8.0 Hz), 6.43–6.30 (3H, m), 6.67 (2H, d, *J* = 12.0 Hz), 3.43 (2H, d, *J* = 8.0 Hz), 3.10 (2H, t, *J* = 8.0 Hz), 3.04–2.93 (4H, m), 1.82–1.66 (4H, m), 1.67–1.58 (2H, m), 1.04–0.91 (1H, m), 0.89–0.73 (1H, m), 0.51 (3H, t, *J* = 8.0 Hz). ¹³C NMR (DMSO-*d*₆, 75 MHz): δ 180.57, 158.25, 150.74, 142.47, 131.93, 129.72, 127.58, 123.00, 121.49, 109.16, 107.49, 107.01, 103.16, 54.86, 52.97, 50.32, 45.38, 36.39, 30.13, 23.06, 21.24, 8.37. LCMS (ESI) RT: 4.98 min, *m/z*: 394.2 [M+H]⁺ at 210 and 254 nm. R_f: 0.1 (EtOAc). HRMS (ESI) [MH] calcd. for C₂₄H₃₁N₃O₂ 393.2654, found 393.2652.

3-Ethyl-3-{4-[4-(4-methylphenyl)piperazin-1-yl]butyl}-1,3-dihydro-2H-indol-2-one (3, Cimbi-772)

1-(4-Methylphenyl)piperazine (210 mg, 1.192 mmol), sodium carbonate (126 mg, 1.192 mmol) and 3-(4-chlorobutyl)-3-ethyloxindole (300 mg, 1.192 mmol) yielded in (**3**) (312 mg, 0.797 mmol, 67%) as a white solid. Compound (**3**) was purified by chromatography using EtOAc as the eluent. Mp 127.8–128.3 °C. ¹H NMR (CDCl₃, 400 MHz): δ 9.28 (1H, s), 7.19 (1H, m), 7.12 (1H, m), 7.05 (3H, m), 6.91 (1H, d, *J* = 7.8 Hz), 6.82 (2H, m), 3.10 (4H, m), 2.52 (4H, m), 2.26 (5H, m), 1.94 (2H, m), 1.80 (2H, m), 1.43 (2H, m), 1.13 (1H, m), 0.93 (1H, m), 0.64 (3H, t, *J* = 7.4 Hz). ¹³C NMR (CDCl₃, 75 MHz): δ 182.8, 149.1, 141.5, 132.5, 129.5, 129.0, 127.5, 122.9, 122.2, 116.2, 109.5, 58.2, 54.2, 53.1, 49.5, 37.5, 30.9, 26.8, 22.2, 20.3, 8.0. LCMS (ESI) RT: 5.36 min, *m/z* 392.1 [M+H]⁺ at 210 and 254 nm. R_f: 0.12 (EtOAc). HRMS (ESI) [MH]⁺ calcd. for C₂₅H₃₄N₃O 392.269, found 392.2710.

3-{4-[4-(4-Chlorophenyl)piperazin-1-yl]butyl}-1,3-dimethyl-1,3-dihydro-2H-indol-2-one (22)

To a mixture of *n*-BuLi in hexane (2.5 M, 0.732 mL, 1.83 mmol) and dry THF (10 mL), a solution of **20** (352 mg, 0.92 mmol) in dry THF (10 mL) was added dropwise at –78 °C, under argon atmosphere. Then MeI (0.014 g, 0.10 mmol) was added dropwise, and the reaction mixture was allowed to warm to room temperature. The stirring was continued for 12 additional hours, the mixture was quenched with ethanol (20 mL), and the solvents were evaporated. The residue was dissolved in ethyl acetate and extracted with water. The organic layer was dried over Na₂SO₄ and

evaporated. The oily residue was purified by column chromatography using EtOAc/Et₃N (300:3) as the eluent to yield 125 mg (0.30 g, 53%) as a white solid. ¹H NMR (CDCl₃, 300 MHz): δ 7.25 (1H, t, J = 6.0 Hz), 7.18-7.15 (3H, m), 7.05 (1H, t, J = 6.0 Hz), 6.81 (3H, t, J = 9.0 Hz), 3.20 (3H, s), 3.10 (4H, t, J = 6.0 Hz), 2.49 (4H, t, J = 6.0 Hz), 2.24 (2H, t, J = 9.0 Hz), 1.98-1.88 (1H, m), 1.80-1.70 (1H, m), 1.46-1.33 (2H, m), 1.35 (3H, s), 1.04-0.83 (2H, m). R_f = 0.28 (EtOAc/Et₃N 250:3).

3-{4-[4-(4-Chlorophenyl)piperazin-1-yl]butyl}-3-(2-fluoroethyl)-1,3-dihydro-2H-indol-2-one (23)

To a mixture of *n*-BuLi in hexane (2.5 M, 0.52 mL, 1.30 mmol) and dry THF (5 mL), the solution of **20** (200 mg, 0.52 mmol) in dry THF (10 mL) was added dropwise at -78 °C, under argon atmosphere. Then 1-bromo-2-fluoroethane (0.164 g, 1.30 mol) was added dropwise, and the reaction mixture was allowed to warm to room temperature. The stirring was continued for 12 additional hours, the mixture was quenched with ethanol (20 mL), and the solvents were evaporated. The residue was dissolved in ethyl acetate and extracted with water. The organic layer was dried over Na₂SO₄ and evaporated. The oily residue was purified by column chromatography using EtOAc/Et₃N (300:3) as the eluent to yield 50 mg (0.12 mmol, 24%) as a white solid. Mp 123–124 °C. ¹H NMR (CDCl₃, 300 MHz): δ 9.14 (1H, s), 7.24–7.11 (4H, m), 7.03 (1H, m), 6.89 (1H, d, J = 6.0 Hz), 6.76 (2H, d, J = 9.0 Hz), 4.31 (1H, m), 4.16 (1H, m), 3.08 (4H, t, J = 6.0 Hz), 2.48 (4H, t, J = 6.0 Hz), 2.44–2.33 (1H, m), 2.23 (2H, t, J = 6.0 Hz), 2.17–2.00 (1H, m), 1.97–1.91 (1H, m), 1.86–1.76 (1H, m), 1.52–1.30 (2H, m), 1.19–1.05 (1H, m), 0.97–0.86 (1H, m). ¹³C NMR (CDCl₃, 75 MHz): δ 182.20, 149.98, 141.39, 131.49, 129.04, 128.30, 124.58, 123.38, 122.65, 117.31, 110.18, 80.77 (d, J = 140 Hz), 58.22, 53.09, 51.25, 49.14, 38.16, 37.89, 26.88, 21.94. LCMS (ESI) RT: 2.66 min, m/z: 430.29 [M+H]⁺ at 210 and 254 nm. R_f = 0.25 (EtOAc/Et₃N 250:3). HRMS (ESI) [MH⁺] calcd. for C₂₄H₃₀ClFN₃O 430.2055, found 430.2069.

***tert*-Butyl 3-ethyl-3-{4-[4-(3-hydroxyphenyl)piperazin-1-yl]butyl}-2-oxo-2,3-dihydro-1H-indole-1-carboxylate (11)**

To a solution of **10** (0.520 g, 1.323 mmol) in dry DMF (10 mL) was added NaH (36 mg, 1.523 mmol) and TBDPSCl (0.971 g, 1.323 mmol). The resulting mixture was stirred overnight at 110 °C and then poured into water, and extracted with ethyl acetate. The combined organic layers were washed 3 times with water, then with brine, dried over MgSO₄, and concentrated in vacuo to afford

(**27a**). The crude mixture was used without further purification. LC-MS (ESI) m/z : 632.5; RT: 6.75 min. R_f : 0.7 (EtOAc/MeOH 10:0.3).

Afterwards, (**27a**) (1.323 mmol) was dissolved in dry THF, cooled to $-5\text{ }^{\circ}\text{C}$, 1 M NaHMDS (1.323 mL, 1.323 mmol) was added and the mixture was stirred for 30 min. Boc_2O (275 mg, 1.323 mmol) was added and stirred for 1 h. Excess NaHMDS was quenched with a AcOH:THF 1:4 mixture (6 mL), then with water (40 mL). Extraction was performed with EtOAc (3×10 mL). The combined organic layers were washed with brine (2×10 mL), dried, concentrated *in vacuo* to yield crude **27**, which was used without further purification. LC-MS (ESI) m/z : 732.6; RT: 7.12 min; R_f : 0.7 (EtOAc/MeOH 10:0.3).

Finally, **27** (1.323 mmol) and NH_4F (0.23 g, 3.30 mmol) was dissolved in dry MeOH (10 mL) and heated at $70\text{ }^{\circ}\text{C}$ for 30 min. Afterwards, the solvent was removed, the residue was dissolved in NH_4OH (7 mL) and extracted 3 times with CHCl_3 . The combined organic layers were dried over Na_2SO_4 and evaporated. The crude oil was purified with column chromatography using EtOAc/heptane (1:1) as the eluent to yield **21** (0.83 g, 1.68 mmol, 51%) as a white solid. Mp $68\text{--}69\text{ }^{\circ}\text{C}$. ^1H NMR (CDCl_3 , 300 MHz): δ 7.81 (1H, d, $J = 5\text{ Hz}$), 7.34–7.27 (1H, m), 7.18–7.04 (3H, m), 6.45–6.42 (1H, m), 6.34–6.31 (2H, m), 3.18 (4H, t, $J = 6.0\text{ Hz}$), 2.65 (4H, t, $J = 6.0\text{ Hz}$), 2.37 (2H, t, $J = 6.0\text{ Hz}$), 1.97–1.89 (2H, m), 1.82–1.71 (2H, m), 1.66 (9H, s), 1.55–1.39 (2H, m), 1.13–0.79 (2H, m), 0.62 (3H, t, $J = 6.0\text{ Hz}$). ^{13}C NMR (CDCl_3 , 75 MHz): δ 179.16, 171.60, 157.66, 152.17, 149.17, 139.95, 130.80, 127.97, 124.60, 122.66, 114.81, 108.01, 107.57, 103.66, 84.41, 68.63, 57.74, 53.97, 52.52, 48.20, 38.10, 33.42, 32.08, 28.15, 25.78, 22.19, 8.60. LCMS (ESI) RT: 5.60 min, m/z : 494.4 $[\text{M}+\text{H}]^+$ at 210 and 254 nm. $R_f = 0.25$ (EtOAc/heptane 1:1). HRMS (ESI) $[\text{MH}^+]$ calcd. for $\text{C}_{29}\text{H}_{40}\text{N}_3\text{O}_4$ 494.3013, found 494.3031.

Remark: Unfortunately, a direct protection approach with Boc_2O and Na_2CO_3 did not lead to any success. This is in contrast to a reported procedure for unsubstituted oxindoles [4].

***tert*-Butyl 3-ethyl-3-{4-[4-(3-methoxyphenyl)piperazin-1-yl]butyl}-2-oxo-2,3-dihydro-1*H*-indole-1-carboxylate (**28**)**

Cimbi-775 (20 mg, 0.049 mmol) was dissolved in dry THF and cooled to $-5\text{ }^{\circ}\text{C}$. 1 M NaHMDS solution (0.049 mL, 0.049 mmol) was added and the mixture was stirred for 30 min. Boc_2O (10.24 mg, 0.049 mmol) was added and stirring was continued for 1 h. The excess of NaHMDS was quenched with a AcOH:THF 1:4 solution (6 mL), then with water (40 mL). Extraction was

performed with EtOAc (3×10 mL). The combined organic layers were washed with brine (2×10 mL), dried and concentrated in vacuo to yield in crude (**28**). LCMS (ESI) RT: 6.07 min, m/z: 508.4 [M+H]⁺ at 210 and 254 nm.

3-{4-[4-(4-Bromophenyl)piperazin-1-yl]butyl}-3-ethyl-1,3-dihydro-2H-indol-2-one (7)

1-(4-Bromophenyl)piperazine (479 mg, 1.986 mmol), 3-(4-chlorobutyl)-3-ethyloxindole (500 mg, 1.98 mmol) and Na₂CO₃ (211 mg, 1.986 mmol) were heated to 180 °C and stirred for 3 h. After cooling to room temperature the resulting solid was dissolved in a mixture of EtOAc and water. The organic layer was concentrated in vacuo and purified using flash chromatography (EtOAc). Yield: 557.2 mg (62%). Mp 145.0–145.5 °C. ¹H NMR (CDCl₃, 400 MHz): δ 7.73 (1H, s), 7.33 (2H, m), 7.21 (1H, td, J = 7.59, 1.38 Hz), 7.12 (1H, m), 7.06 (1H, m), 6.88 (1H, d, J = 7.78 Hz), 6.76 (2H, m), 3.16 (4H, m), 2.56 (4H, bs), 2.31 (2H, t, J = 7.65 Hz), 1.93 (2H, m), 1.79 (2H, m), 1.45 (2H, m), 1.12 (1H, m), 0.93 (1H, m), 0.64 (3H, t, J = 7.40 Hz). ¹³C NMR (CDCl₃, 75 MHz): δ 181.8, 150.2, 141.1, 132.5, 131.8, 127.6, 123.2, 122.5, 117.6, 109.3, 58.1, 54.10, 52.8, 48.7, 37.5, 31.1, 26.9, 22.2, 8.5. LCMS (ESI): RT: 5.97 min, m/z: 457.2 [M+H]⁺ at 210 and 254 nm. R_f = 0.18 (EtOAc). HRMS (ESI) [MH] calcd. for C₂₄H₃₁BrN₃O 456.1645, found 456.1657.

3-Ethyl-3-(4-{4-[4-(4,4,5,5-tetramethyl-1,3,2-dioxaborolan-2-yl)phenyl]piperazin-1-yl}butyl)-1,3-dihydro-2H-indol-2-one (8)

7 (77 mg, 0.169 mmol), KOAc (19.8 mg, 0.202 mmol), bis(pinacolato)diboron (86 mg, 0.337 mmol) and Pd(dddppf)Cl₂ (10 mg, 0.01 mmol) were dissolved in dry dioxane (10 mL), heated to 100 °C and stirred for 12 h. The reaction was then cooled to room temperature, stirred with brine (10 mL) for 10 min and extracted with EtOAc (3×50 mL). The combined organic layers were dried, concentrated in vacuo and purified by column chromatography using heptane and ethyl acetate to yield 43 mg (51%) as a dark yellow oil. ¹H NMR (CDCl₃, 400 MHz): δ 7.70 (2H, d, J = 8.78 Hz), 7.59 (1H, s), 7.20 (1H, td, J = 7.65, 1.38 Hz), 7.13 (1H, m), 7.07 (1H, td, J = 7.40, 0.88 Hz), 6.87 (3H, m), 3.24 (4H, t, J = 4.77 Hz), 2.52 (4H, bs), 2.27 (2H, t, J = 7.53 Hz), 1.93 (2H, m), 1.79 (2H, m), 1.44 (2H, m), 1.33 (12H, s), 1.12 (1H, m), 0.92 (1H, m), 0.64 (3H, t, J = 7.40 Hz). ¹³C NMR (CDCl₃, 75 MHz): δ 182.3, 153.23, 141.2, 136.1, 132.6, 127.6, 123.1, 122.5, 114.3, 109.4, 83.4, 58.1, 54.2, 52.8, 47.8, 37.5, 31.1, 24.8, 24.6, 22.3, 8.5. LC-MS (ESI): RT: 7.00 min, m/z: 504.3 [M+H]⁺ at 210 and 254 nm. R_f = 0.73 (EtOAc). HRMS (ESI) [MH⁺] calcd. for C₃₀H₄₃BN₃O₃ 504.3397, found 504.3420.

5. Chiral resolution of Cimbi-772 (3) and Cimbi-775 (4)

Analytical resolution: 5 μ L of the desired racemate (1 mg/1 mL MeCN) were injected on a Lux 5 μ m Cellulose-4 LC Column 250 x 4.6 mm. The sample was eluted with 20mM AmBi: MeCN:DEA (40:60:0.1) with a flowrate of 1 mL/min. 1) Retention time (RT) of the separated enantiomers of Cimbi.772: a) 12.45 min b) 16.81 min 2) RT of the enantiomers of Cimbi-775: a) 11.956 min b) 14.13 min-

Chiral separation was carried out using a Jasco PU 880 pump, a spectraseries UV100 detector connected to a Merck Hitachi D-2000 chromatointegrator and a Diacel Chiralpak IF (5 μ m 10 mm x 250 mm) column. Cimbi-772 was separated using heptane:IPA:DEA 90:10:0.1 at 4.5 mL/min and Cimbi-775 was separated using heptane:IPA:DEA 80:20:0.1 at 4.5 mL/min.

a) Optical Rotation

Optical rotation was measured on a Bellingham + Stanley ADP410 polarimeter at 689 nm.

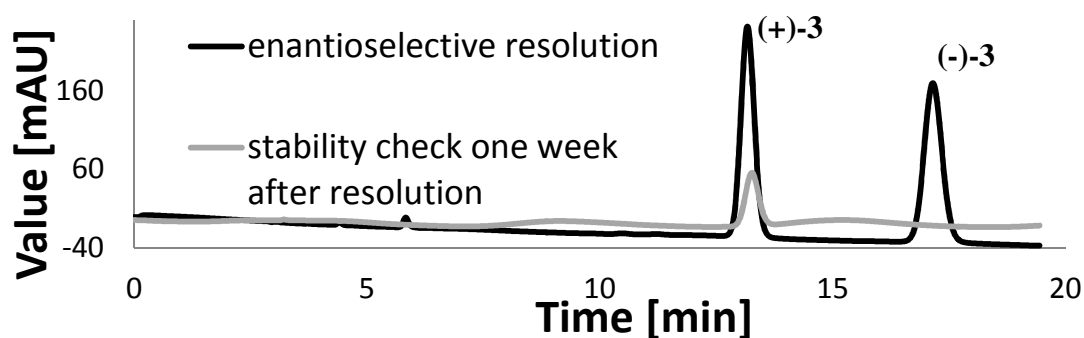
(-)-3: $[\alpha]_D^{20} = -16$ (c = 0.5, CHCl₃)

(+)-3: $[\alpha]_D^{20} = +16$ (c = 0.5, CHCl₃)

(-)-4: $[\alpha]_D^{20} = -16$ (c = 0.5, CHCl₃)

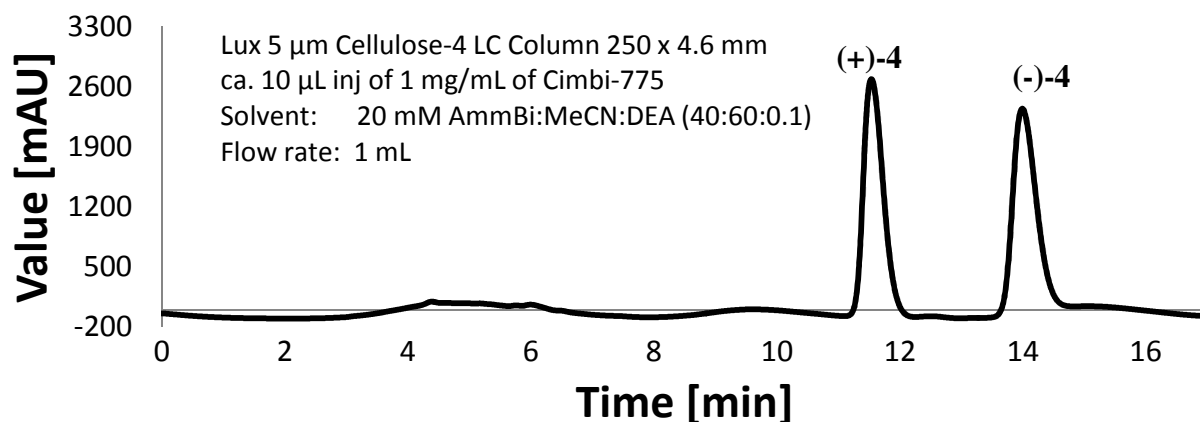
(+)-4: $[\alpha]_D^{20} = +16$ (c = 0.5, CHCl₃)

b) Chiral resolution of Cimbi-772 (3) and stability test

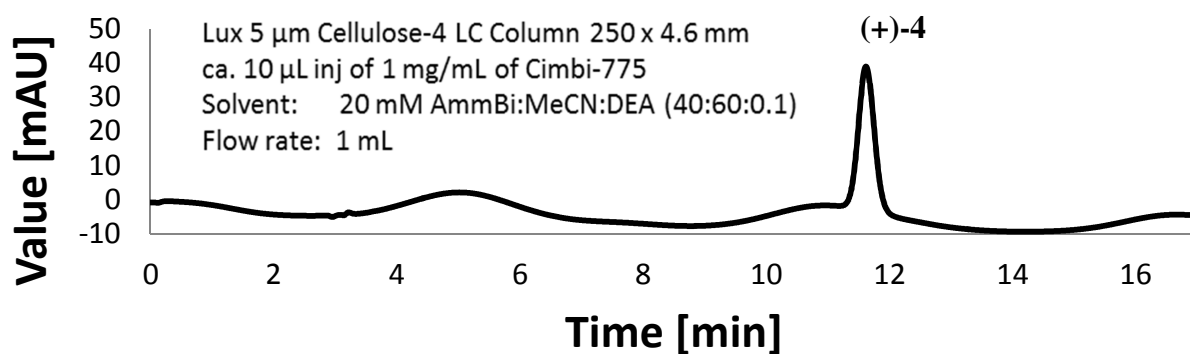


Chiral resolution and stability test of one enantiomer of Cimbi-772, the same HPLC conditions as above were used

c) Chiral resolution of Cimbi-775 (4)



d) Stability test of (+)-4



6. PDSP Screening

In vitro radioligand binding assays were performed by the NIMH Psychoactive Drug Screening Program at the Department of Biochemistry, Case Western Reserve University, Cleveland, Ohio, USA (Bryan Roth, Director). Compounds Cimbi-712, Cimbi-717, Cimbi-772, (+)-**3**, Cimbi-775 and (+)-**4** were assayed for their affinities for a broad spectrum of receptors and transporters in competitive binding experiments in vitro using cloned human receptors. Reported values of the inhibition coefficient (K_i) are mean \pm SD of four separate determinations.

7. Receptor distribution of colocalized targets

Table S2 shows the receptor Distribution of colocalized Targets. B_{max} values are reported in fmol/mg wet tissue or in fmol/mg protein.

Table S2: Receptor distribution of colocalized targets

	5-HT ₇ ^[5]	5-HT _{1A} ^[6, 7]	5-HT _{2A} ^[8]	α ₁	H ₁ ^[9]	sigma ^[10]	SERT ^[8]
cortex	2.3	73	56	283 ^[11]	14	101	4.3
Hippocampus	5.7	82	24	234 ^[12]	6.4	73	2.6
thalamus	12	4	6	88 ^[12]	4	58	10

8. Selectivity/B_{max} ratio for 5-HT₇

Table S3: Selectivity/B_{max} ratio for 5-HT₇ of the compounds relative to other relevant targets in different brain regions. Data are based on values reported in Table 1 and Table S2. Human B_{max} values were used.

$$\text{Selectivity/B}_{\text{max}} \text{ ratio} = \left(\frac{K_{d,\text{off-target}}}{K_{d,\text{target}}} \right) \left(\frac{B_{\text{avail,target}}}{B_{\text{avail,off-target}}} \right)$$

		versus 5-HT _{1A}	versus 5-HT _{2A}	versus α ₁	versus H1	versus sigma	versus SERT
Cimbi-775 (4)	cortex	0.3	0.5	0.5	17.8	0.15	17
	hippocampus	0.7	2.9	1.4	-	0.42	70
	thalamus	32	25	7.6	193	1.11	38
(+)-4	cortex	0.5	1.3	7.5	1.05	0.09	18
	hippocampus	1.2	7.6	22	-	0.32	74
	thalamus	52	64	123	11	0.86	41
Cimbi-717 (2)	cortex	0.5	1.3	0.2	6.0	0.2	18
	hippocampus	1.2	7.5	0.5	-	0.61	73
	thalamus	52	63	3.0	67	1.6	40
Cimbi-772 (3)	cortex	2.3	0.2	0.5	22	0.12	24
	hippocampus	5	1.4	1.6	-	0.4	99
	thalamus	216	12	9.0	244	1.1	54
(+)-3	cortex	4.4	0.6	1.3	6.6	0.1	25
	hippocampus	9.7	3.9	4.1	-	0.5	106
	thalamus	421	34	23	72	1.2	58
Cimbi-712 (1)	cortex	3.7	0.4	0.2	21.8	0.24	14
	hippocampus	8.3	2.0	0.6	-	0.85	59
	thalamus	359	17.1	3.4	236	2.2	32

Remark: Exemplarily, we would like to calculate one selectivity/B_{max} ratio for Cimbi-712 in thalamus for the target (5-HT₇) and for the off-target (5-HT_{1A}): The affinity of Cimbi-712 for the 5-HT₇ receptor is 4.1 nM and for the 5-HT_{1A} receptor, it is 491 nM (Table 1 and Table S3). B_{avail}/B_{max} in thalamus is 12 fmol/mg original wet tissue for the 5-HT₇ receptor and 4 fmol/mg original wet tissue for the 5-HT_{1A} receptor.

$$\text{selectivity/Bmax ratio}_{5\text{-HT}_7/5\text{-HT}_{1A}} = S \times D = \left(\frac{491 \text{ nM}}{4.1 \text{ nM}} \right) \left(\frac{12 \frac{\text{fmol}}{\text{mg wet tissue}} \text{ 5-HT}_7 \text{ receptor}}{4 \frac{\text{fmol}}{\text{mg wet tissue}} \text{ 5-HT}_{1A} \text{ receptor}} \right) = 359.26 \frac{5\text{-HT}_7}{5\text{-HT}_{1A}}$$

Thus, the selectivity/B_{max} ratio of Cimbi-712 for 5-HT₇ in thalamus is 359-fold relative to the 5-HT_{1A} receptor. Of course, one should critically review the selectivity/B_{max} ratio. The original in vitro data can vary considerably due to different determination methods. In addition, it is important to remember that in vitro binding characteristics may not always predict in vivo binding characteristics. That is, because radioligands which are suitable for in vitro quantification may not necessarily be ideal for in vivo PET imaging. PET tracers have to enter the brain through the blood–brain barrier (BBB). The tracer can be a substrate of efflux pumps. Metabolism or pharmacokinetics could further limit its use [13]. Nonetheless, when taken these pre-considerations into account, the selectivity/B_{max} ratio is a good estimate of the in vivo binding of a given compound.

9. In vitro characterization

Cell culture and cAMP accumulation assay

HeLa cells stably expressing the human 5-HT_{7(a)} receptor [HeLa h5-HT_{7(a)}; kindly provided by Dr. Mark Hamblin] were used to determine activity of the test compounds in vitro. We have previously described the pharmacological profile of HeLa h5-HT_{7(a)} and recently used these cells to characterize novel ligands of 5-HT₇ [14, 15]. Cells were cultured in a standard incubator at 37°C and 5% CO₂/95% air. Growth medium consisted of DMEM supplemented with 10% fetal bovine serum, 2 mM L-glutamine and 250 µg/ml Geneticin (G418). Cells were seeded into 96-well plates (Sarstedt, Helsingborg, Sweden) at a density of 20,000 cells per well 24 hours before experiments. About 18 hours prior to treatment, cells were switched to serum-free medium (DMEM supplemented with 2 mM L-glutamine). All drug solutions were freshly prepared on the day of a given experiment, either from powder (5-HT, pargyline, theophylline) or from 10 mM stocks in DMSO (test compounds). Serial dilutions of the test compounds were prepared in ddH₂O. The final concentration of DMSO was 1% (v/v) at the highest concentration of test compounds, and 1%

DMSO was used as a vehicle control in all experiments. To test for agonist activity, cells were treated with 10 μM of test compounds for 15 minutes. To test for antagonist activity, cells were treated with 1 μM 5-HT for 15 minutes in the absence or presence of increasing concentrations of test compounds. Untreated cells were used to establish baseline concentrations of cAMP in all experiments. To prevent degradation of 5-HT and cAMP, all wells contained a final concentration of 5 μM pargyline and 2.5 mM theophylline. After 15 minutes of treatment, cells from each well were harvested and lysed in 100 μl of 0.1 M HCl containing 1% (v/v) Triton X-100. Intracellular concentrations of cAMP were measured using a kit (cyclic AMP Complete ELISA; Abnova, Taipei City, Taiwan) according to the manufacturer's instructions for acetylated samples.

Determination of antagonist potencies

Results from individual cAMP accumulation assays were normalized (cAMP concentration after treatment with 1 μM 5-HT = 100%) and then pooled to construct concentration-response curves for the test compounds. Nonlinear regression and curve fitting were carried out in GraphPad Prism 5 (GraphPad, La Jolla, USA) using a four-parameter equation, with the top plateau fixed at 100%. Based on the observation of complete antagonism (5-HT-induced cAMP suppressed to baseline) for all four test compounds, the bottom plateau was fixed at the average value of normalized cAMP observed at the highest test compound concentration (100 μM). Inhibitory potencies (IC_{50} values) were derived from nonlinear regression and best-fit curves were plotted.

Additional notes

All cell culture reagents (DMEM, FBS, L-glutamine, Geneticin) were from Life Technologies. DMSO, 5-HT, pargyline and theophylline were from Sigma-Aldrich.

10. Lipophilicity[16]

Lipophilicities were determined using a Dionex Ultimate 3000 UHPLC equipped with degasser, autosampler, column-oven and UV-detector. The eluent was 50:50 (v/v) 20 mM sodium phosphate-buffer (pH = 7.4) and MeOH. Injected volumes were 100 μL with a flow rate of 1 mL/min. The determination was carried out on a Luna C18(2) 5 μm 100 \AA (150 mm \times 4.6 mm, 5 μm) and UV detection was conducted at 254 nm. The logarithm of retention factor of reference compounds (phenol, acetophenone, *p*-cresol, benzene, toluene, chlorobenzene, benzophenone, naphthalene, diphenyl and phenanthrene) and tested compounds was calculated, and a plot of the reference

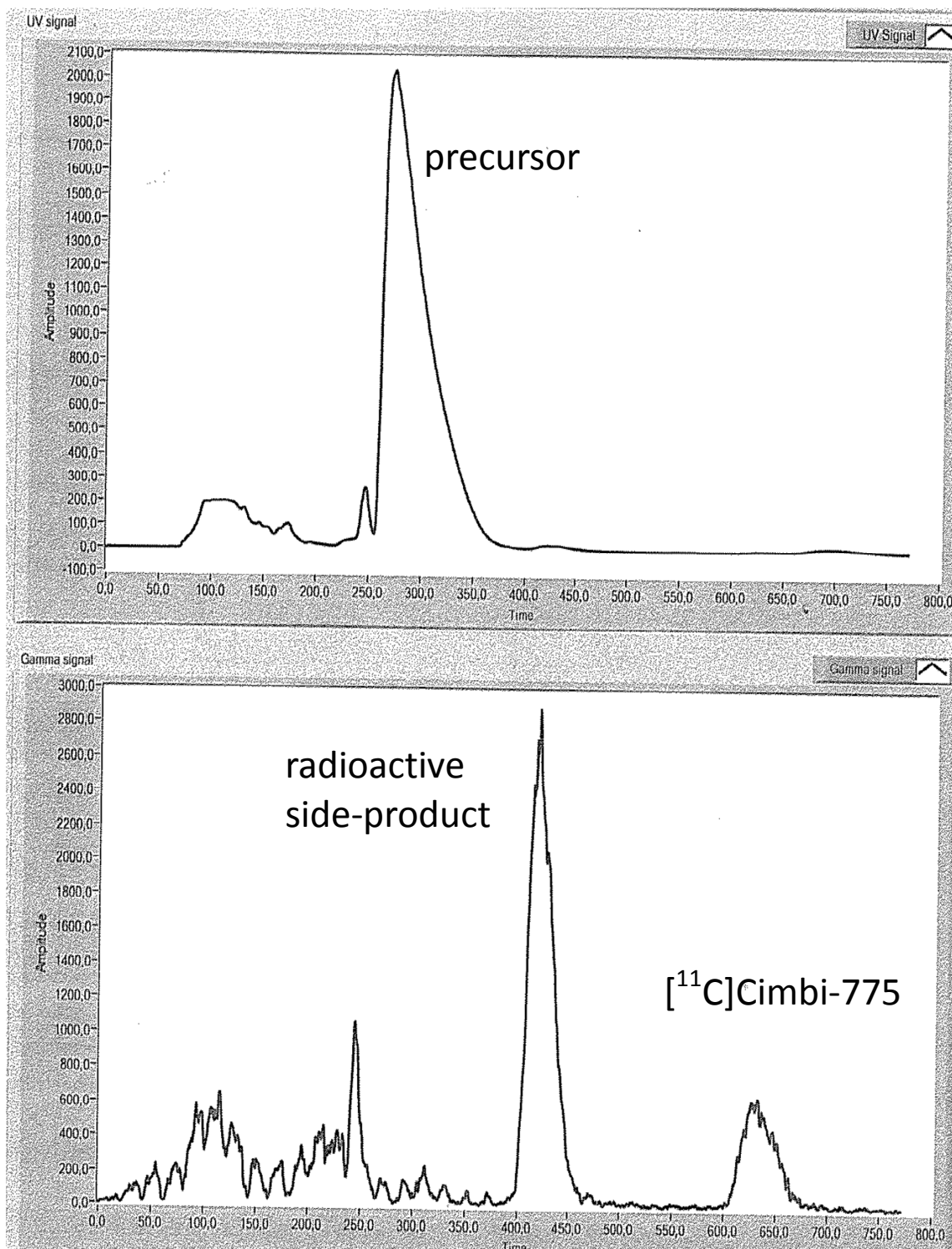
values against their known logD values was used to intrapolate logD values for tested compounds. Lipophilicity data are displayed in Table S1.

Lipophilicity discussion: The development of a successful *in vivo* PET probe for neuroreceptor imaging requires high selectivity for the target, blood-brain-barrier (BBB) passage and a low non-specific binding of the ligand. Especially, the lipophilicity of the compound influences the last two parameters (ideal log $D_{7,4}$ = 2-3 [17]). Therefore, we decided to determine the lipophilicity of our final ligands and to compare them to previously published oxindoles which bear no alkyl moiety at the 3-position [2]. Calculated log $D_{7,4}$ values are displayed in Table 1.

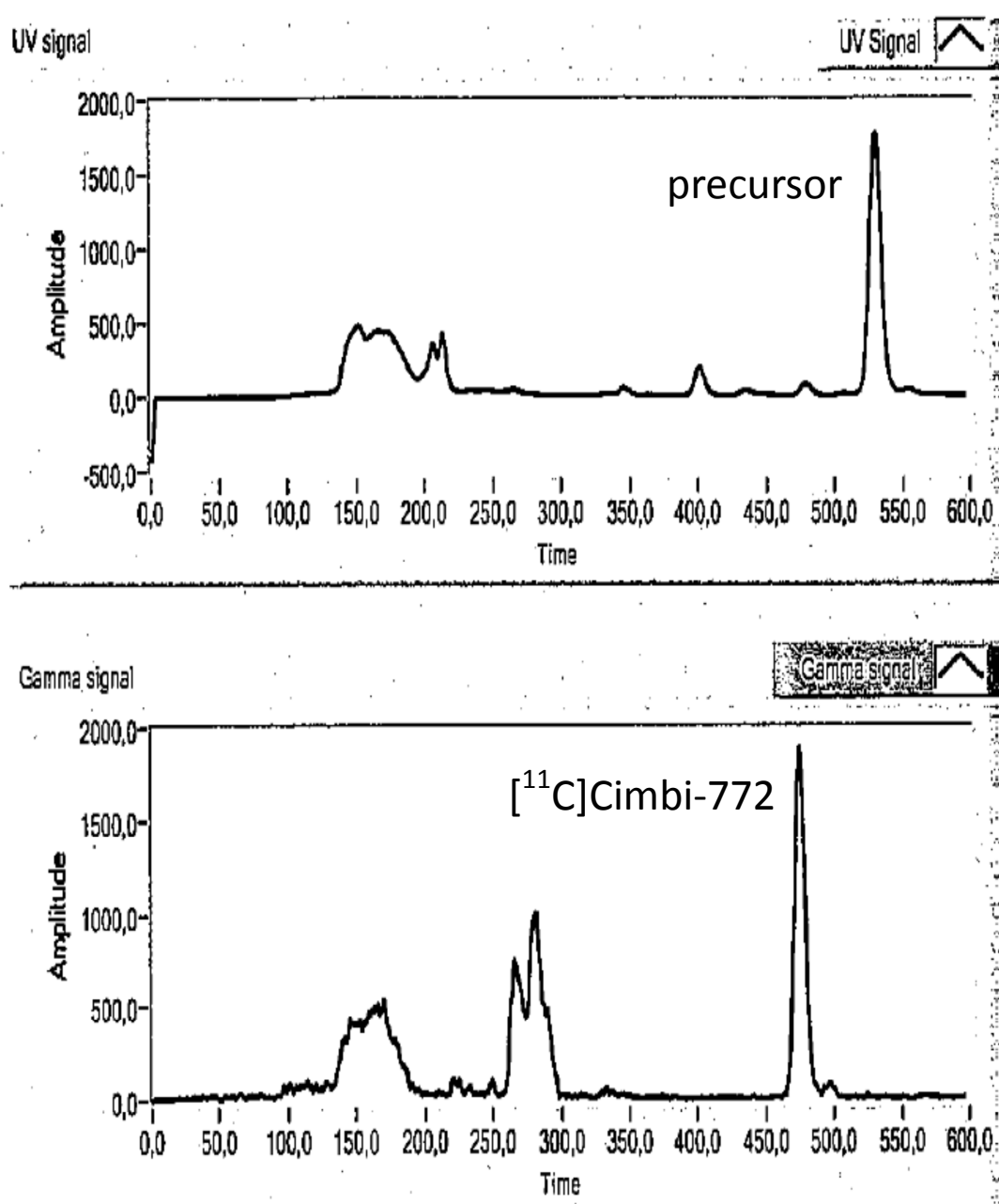
C-3 alkylation increased the log $D_{7,4}$ value about a factor of ~ 0.5 per additional carbon atom. Respectively, different BBB passage and non-specific binding of these alkylated oxindole ligands could be expected and possibly change imaging properties in regards to PET. However, the determined values were still in a reasonable range to continue with their evaluation process. Further, fluorination (compound **33**) of the ethyl moiety reduced the lipophilicity slightly and as expected, hydroxyl derivatives decreased the lipophilicity by a factor of one compared C-3 ethylated compounds. Finally, N-alkylation increased the lipophilicity dramatically and excluded further use of such compounds for PET.

At this stage, it is worthwhile to comment on the relatively high determined log $D_{7,4}$ values in this study, keeping in mind that the ideal interval for small molecules to penetrate the BBB was reported to be 2-3 [17]. However, in our set-up other known CNS-PET ligands (e.g. MDL 100907, altanserin or WAY 100635) show similarly high values. Therefore, we believe that these compounds may have similarly good properties for molecular imaging.

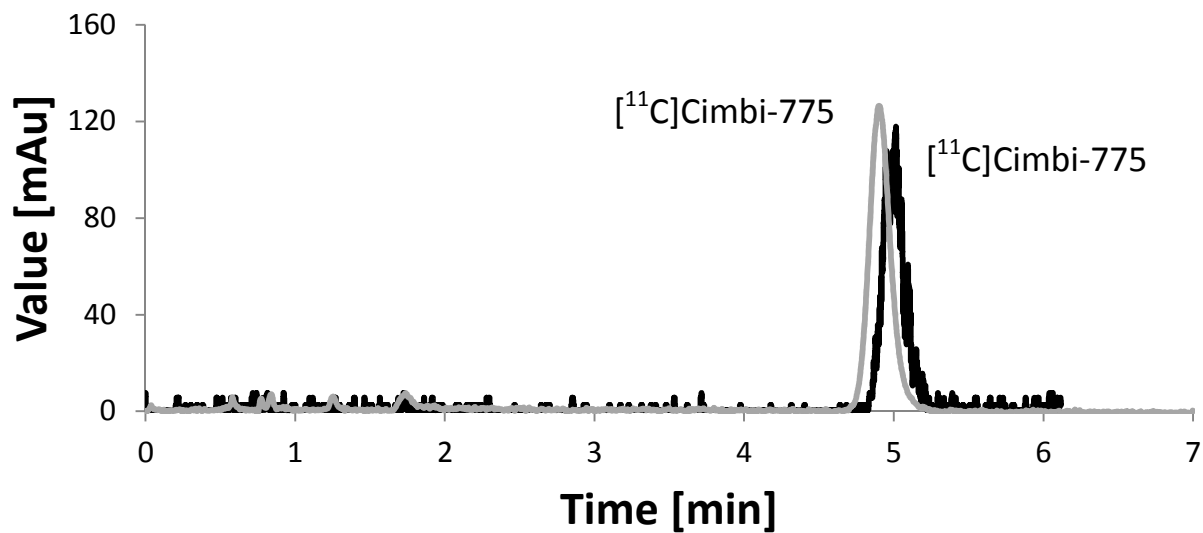
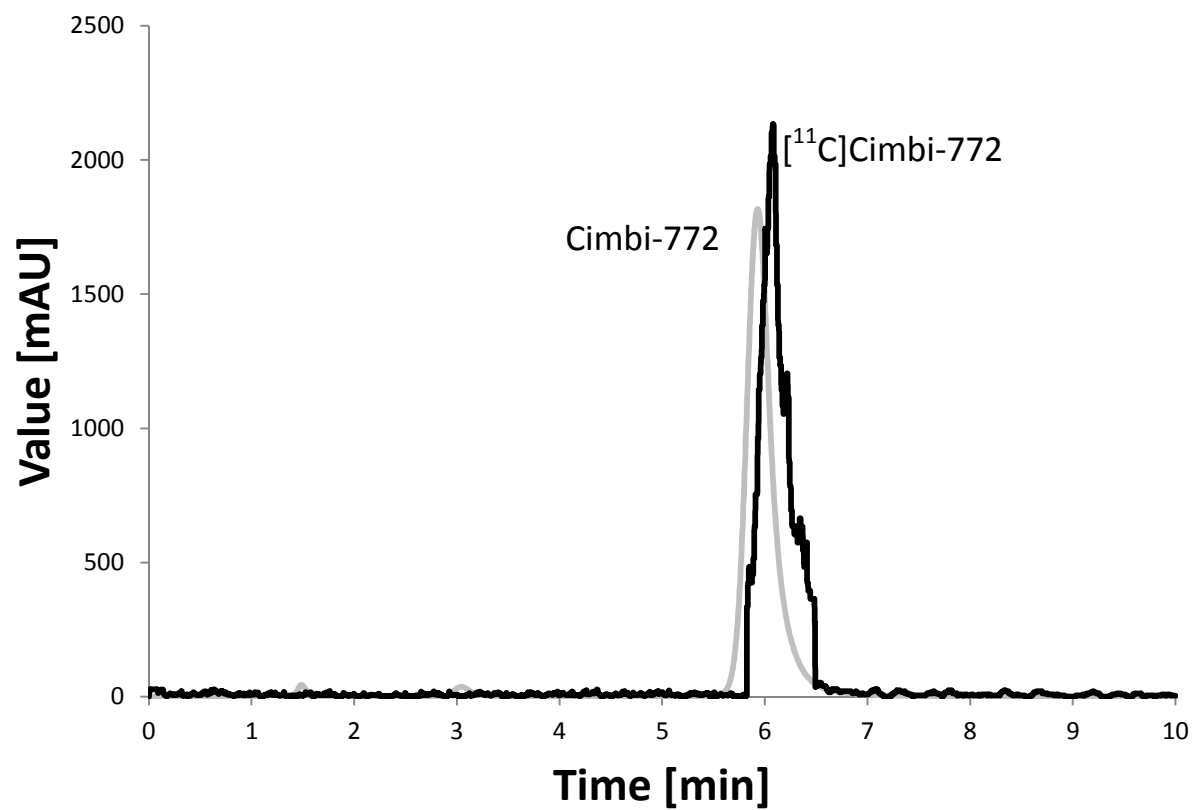
11. Preparative radio-HPLC chromatogram of [^{11}C]Cimbi-775



12. Preparative radio-HPLC chromatogram of [¹¹C]Cimbi-772



13. Analytical HPLC chromatogram of [^{11}C]Cimbi-772 and [^{11}C]Cimbi-775



14. Determination of radiochemical purity and specific radioactivity

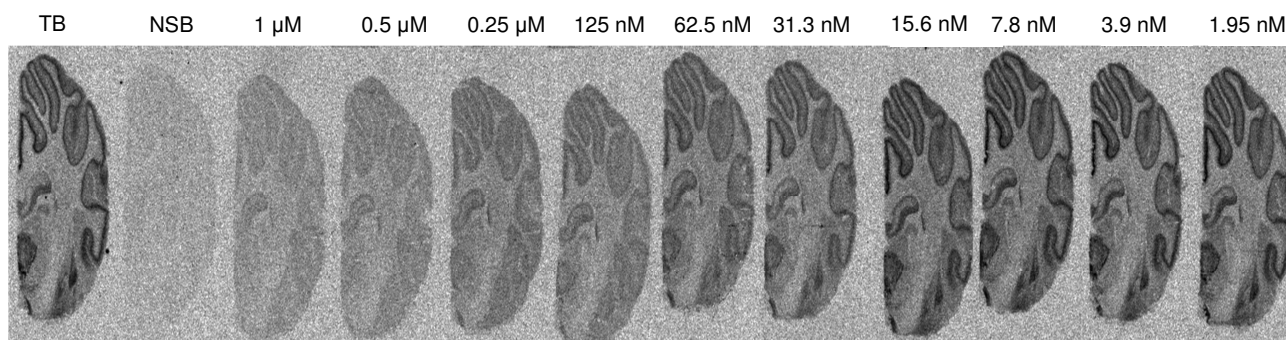
The radiotracer preparation was visually inspected for clarity, and absence of colour and particles. Chemical and radiochemical purities were assessed on the same aliquot by HPLC analysis. Specific activity (A_s) of the radiotracers were calculated from three consecutive HPLC analyses (average) and determined by the area of the UV absorbance peak corresponding to the radiolabeled product on the HPLC chromatogram and compared to a standard curve relating mass to UV absorbance ($\lambda = 225 \text{ nm}$). Column used for [^{11}C]Cimbi-775: Luna 5 μm C18(2) 100Å column (Phenomenex Inc.) (150 x 4.6 mm (50:50 acetonitrile: 0.01M borax buffer; flow rate: 2 mL/min. retention times: [^{11}C]Cimbi-775 = 4.580 min). Column used for [^{11}C]Cimbi-772: Luna 5 μm C18(2) 100Å column (Phenomenex Inc.) (150 x 4.6 mm (50:50 acetonitrile: 0.01M borax buffer; flow rate: 2 mL/min. retention times: [^{11}C]Cimbi-772 = 6.007 min).

15. In vitro autoradiography

a) Competition studies of [^3H]SB-269970 with **3** or **4**

Twenty micrometers coronal sections of pig brain (weight~19 kg) were cut on a HM5000M Cryostat (Microm Intl GmbH) and thawed-mounted on super frost plus glass slides, air-dried and stored at -80°C until use. Sections were cut so both cortical and striatal areas were visible. Autoradiography was performed with 2 nM [^3H]SB-269970 (PerkinElmer, Inc.) and with increasing competing concentrations of **3** and **4** (1.95–1000 nM). Nonspecific binding was determined with 10 μM SB-258719 (Tocris Bioscience). Assay buffer used consistent of 50 mM Tris-HCl, pH 8, and an incubation time of 2 h was used (preincubation 20 min). Sections were washed 3 x 5 min in ice-cold assay buffer with a subsequent dip in ice-cold dH_2O (20 s). Sections were dried and exposed to Fujifilm tritium-sensitive imaging plates for 10 days. Specific radioligand binding (total minus non-specific binding) was plotted as a function of concentration of **3** and **4** and regressed using Prism 4.0 software.

$[^3\text{H}]$ SB-269970 vs Cimbi-772 (3)



$[^3\text{H}]$ SB-269970 vs Cimbi-775 (4)

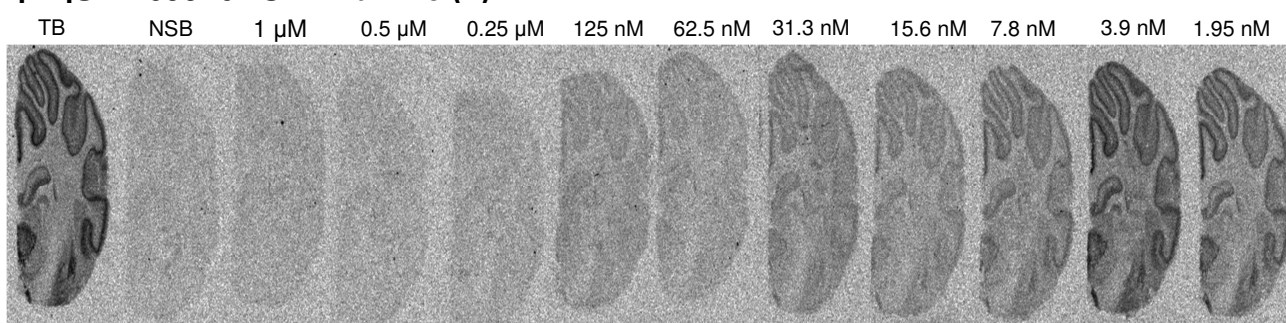


Figure S1: In vitro competition autoradiography images with $[^3\text{H}]$ SB-269970 and several concentrations of **3** or **4**.

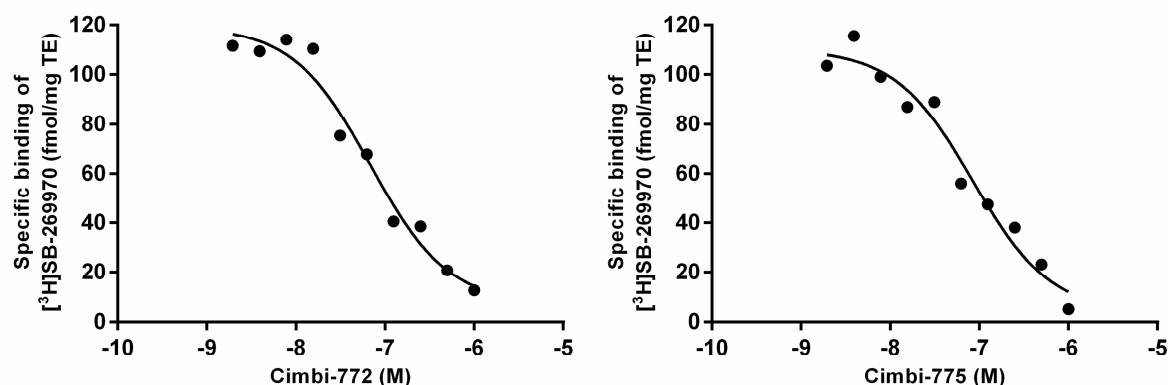


Figure S2: Inhibition of $[^3\text{H}]$ SB-269970 binding to pig brain sections by Cimbi-772 or Cimbi-775.

b) Competition studies of $[^{11}\text{C}]$ Cimbi-775 with SB-269970

Autoradiographic sections were prepared as described before. Autoradiography was performed with 2 nM $[^{11}\text{C}]$ Cimbi-775 and with a competing concentrations of 10 μM SB-269970 (Tocris). Assay buffer used consistent of 50 mM Tris-HCl, pH 7.4, and an incubation time of 1 h was used (preincubation 90 min). Sections were washed 3 x 5 min in ice-cold assay buffer with a subsequent dip in ice-cold dH_2O (20 s). Sections were dried and exposed to Fujifilm tritium-sensitive imaging plates for overnight.

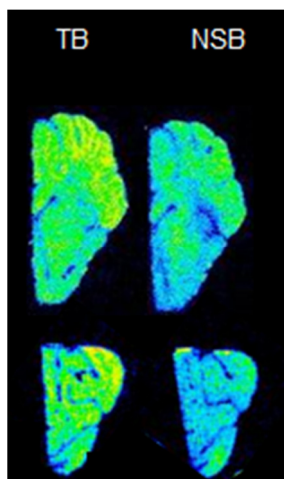


Figure S3: In vitro competition autoradiography images with [^{11}C]Cimbi-775 and one concentrations of SB-269970.

16. Animal procedures

Four female Danish Landrace pigs (mean weight \pm S.D., 18 ± 2.3 kg) were used for in vivo PET imaging. Tranquillization, anaesthesia, monitoring and euthanasia of animals were performed as previously described [19]. All animal procedures were approved by the Danish Council for Animal Ethics (journal no. 2012-15-2934-00156).

17. Quantification of PET data

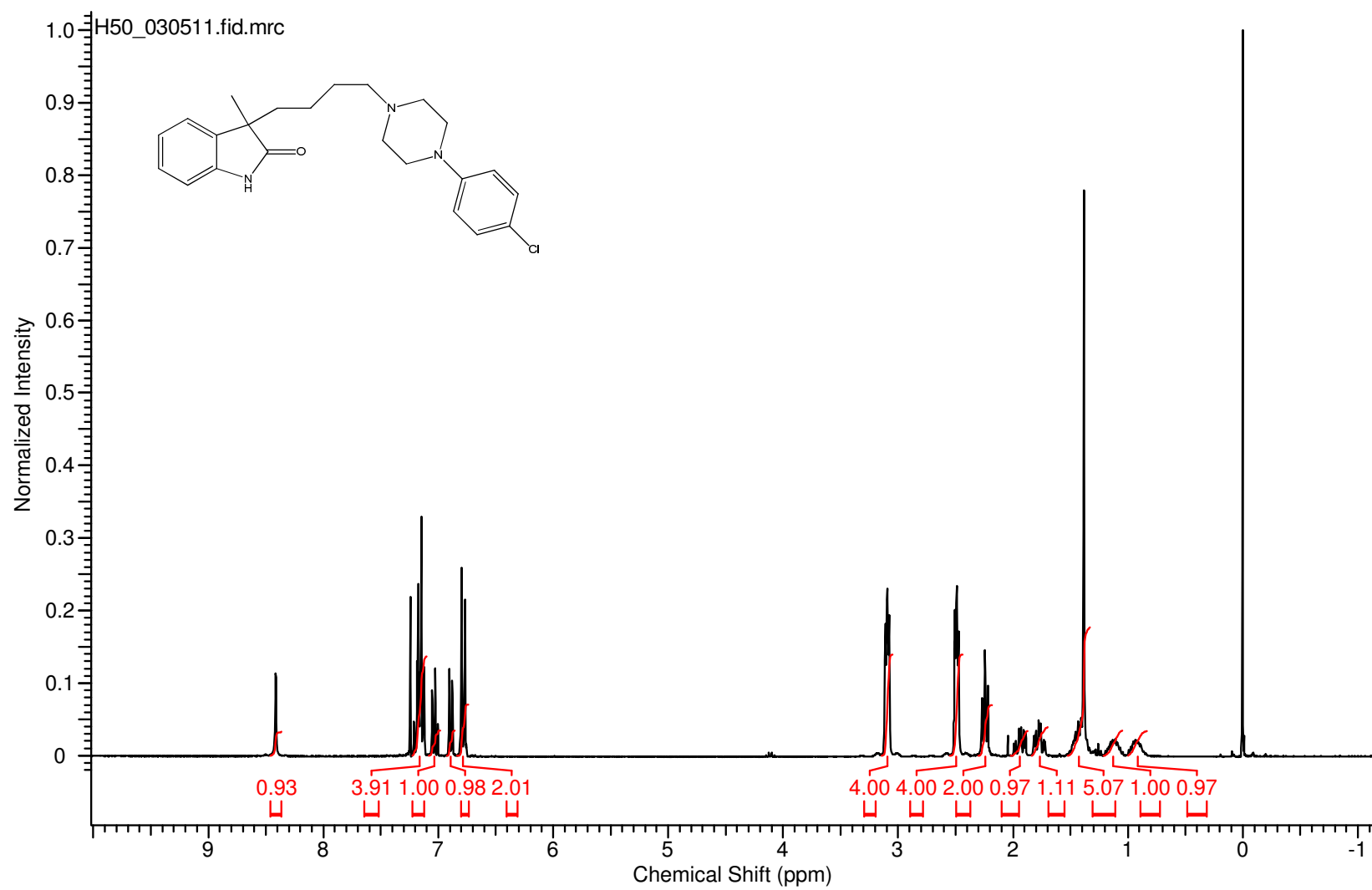
Ninety-minute list-mode PET data were reconstructed into 38 dynamic frames of increasing length (6x10, 6x20, 4x30, 9x60, 2x180, 8x300, and 3x600 seconds). Images consisted of 207 planes of 256×256 voxels of $1.22 \times 1.22 \times 1.22$ mm. A summed picture of all counts in the 90-min scan was reconstructed for each pig and used for co-registration to a standardized MRI-based atlas of the Danish Landrace pig brain, similar to that previously published [18, 19]. The time activity curves (TACs) were calculated for the following volumes of interest (VOIs): cerebellum, cortex, hippocampus, lateral and medial thalamus, caudate nucleus, and putamen. Striatum is defined as the mean radioactivity in caudate nucleus and putamen. The activity in thalamus is calculated as the mean radioactivity in the lateral and medial thalamus. Radioactivity in all VOIs was calculated as the average of radioactive concentration (Bq/mL) in the left and right sides. Outcome measure in the time-activity curves (TACs) was calculated as radioactive concentration in VOI (in kBq/mL) normalized to the injected dose corrected for animal weight (in kBq/kg), yielding standardized uptake values (g/mL).

18. References

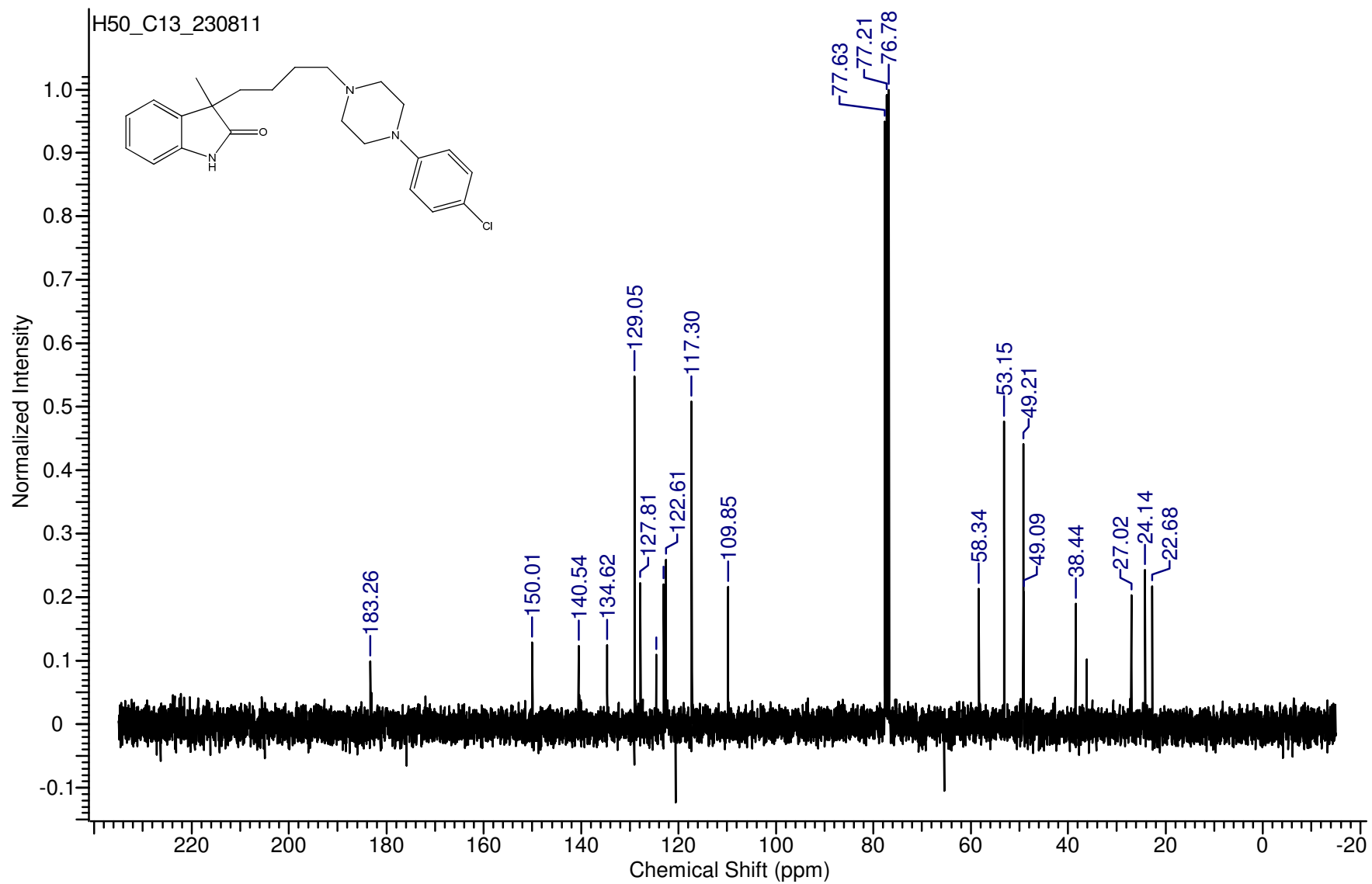
1. Volk, B., et al., *(Phenylpiperazinyl-butyl)oxindoles as selective 5-HT(7) receptor antagonists*. Journal of Medicinal Chemistry, 2008. 51(8): p. 2522-2532.
2. Herth, M.M., et al., *Synthesis and In Vitro Evaluation of Oxindole Derivatives as Potential Radioligands for 5-HT7 Receptor Imaging with PET*. ACS Chem. Neurosci. 2012. 3(12): p. 1002-1007.
3. Andersen, V.L., et al., *Palladium-mediated conversion of para-aminoarylboronic esters into para-aminoaryl-C-11-methanes*. Tetrahedron Letters, 2013. 54(3): p. 213-216.
4. Rajeswaran, W.G. and L.A. Cohen, *Studies on protection of oxindoles*. Tetrahedron, 1998. 54(38): p. 11375-11380.
5. Varnas, K., et al., *Distribution of 5-HT7 receptors in the human brain: a preliminary autoradiographic study using [H-3]SB-269970*. Neuroscience Letters, 2004. 367(3): p. 313-316.
6. Hall, H., et al., *Autoradiographic localization of 5-HT1A receptors in the post-mortem human brain using [H-3]WAY-100635 and [C-11]WAY-100635*. Brain Research, 1997. 745(1-2): p. 96-108.
7. Hall, H., et al., *Whole hemisphere autoradiography of the postmortem human brain*. Nuclear Medicine and Biology, 1998. 25(8): p. 715-719.
8. Varnas, K., C. Halldin, and H. Hall, *Autoradiographic distribution of serotonin transporters and receptor subtypes in human brain*. Human Brain Mapping, 2004. 22(3): p. 246-260.
9. Kanba, S. and E. Richelson, *Histamine H-1-Receptors in Human-Brain Labeled with [Doxepin-H-3]*. Brain Research, 1984. 304(1): p. 1-7.
10. Weissman, A.D., et al., *Sigma-Receptors in Post-Mortem Human Brains*. Journal of Pharmacology and Experimental Therapeutics, 1988. 247(1): p. 29-33.
11. Grossisseroff, R., et al., *Autoradiographic Analysis of Alpha-1-Noradrenergic Receptors in the Human Brain Postmortem - Effect of Suicide*. Archives of General Psychiatry, 1990. 47(11): p. 1049-1053.
12. DePaermentier, F., et al., *Brain alpha-adrenoceptors in depressed suicides*. Brain Research, 1997. 757(1): p. 60-68.
13. Paterson, L.M., et al., *5-HT radioligands for human brain imaging with PET and SPECT*. Medicinal Research Reviews, 2013. 33(1): p. 54-111.
14. Sjogren, B., M.W. Hamblin, and P. Svenningsson, *Cholesterol depletion reduces serotonin binding and signaling via human 5-HT7(a) receptors*. European Journal of Pharmacology, 2006. 552(1-3): p. 1-10.
15. Lacivita, E., et al., *Investigations on the 1-(2-Biphenyl)piperazine Motif: Identification of New Potent and Selective Ligands for the Serotonin(7) (5-HT7) Receptor with Agonist or Antagonist Action in Vitro or ex Vivo*. Journal of Medicinal Chemistry, 2012. 55(14): p. 6375-6380.
16. OECD Guideline for Testing of Chemicals, adopted 30.03.89.
17. Rowley, M., et al., *Effect of plasma protein binding on in vivo activity and brain penetration of glycine/NMDA receptor antagonists*. Journal of Medicinal Chemistry, 1997. 40(25): p. 4053-4068.
18. Kornum, B.R., et al., *Evaluation of the novel 5-HT4 receptor PET ligand [11C]SB207145 in the Gottingen minipig*. J Cereb Blood Flow Metab, 2009. 29(1): p. 186-196.
19. Ettrup, A., et al., *Radiosynthesis and Evaluation of 11C-CIMBI-5 as a 5-HT2A Receptor Agonist Radioligand for PET*. J Nucl Med, 2010. 51(11): p. 1763-1770.

19. Selected analytical data

3-{4-[4-(4-Chlorophenyl)piperazin-1-yl]butyl}-3-methyl-1,3-dihydro-2*H*-indol-2-one (**17**)

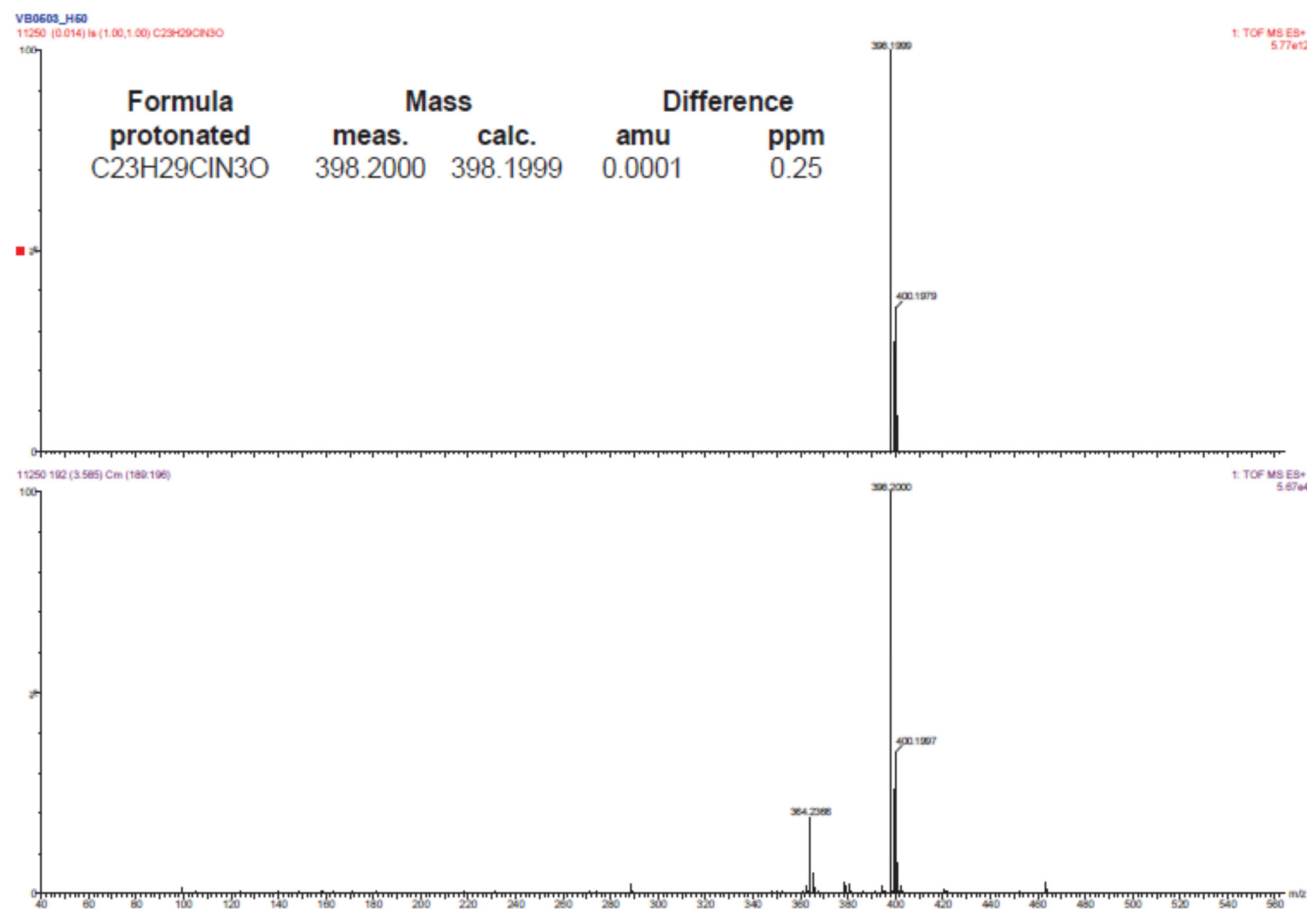


3-{4-[4-(4-Chlorophenyl)piperazin-1-yl]butyl}-3-methyl-1,3-dihydro-2*H*-indol-2-one (**17**)

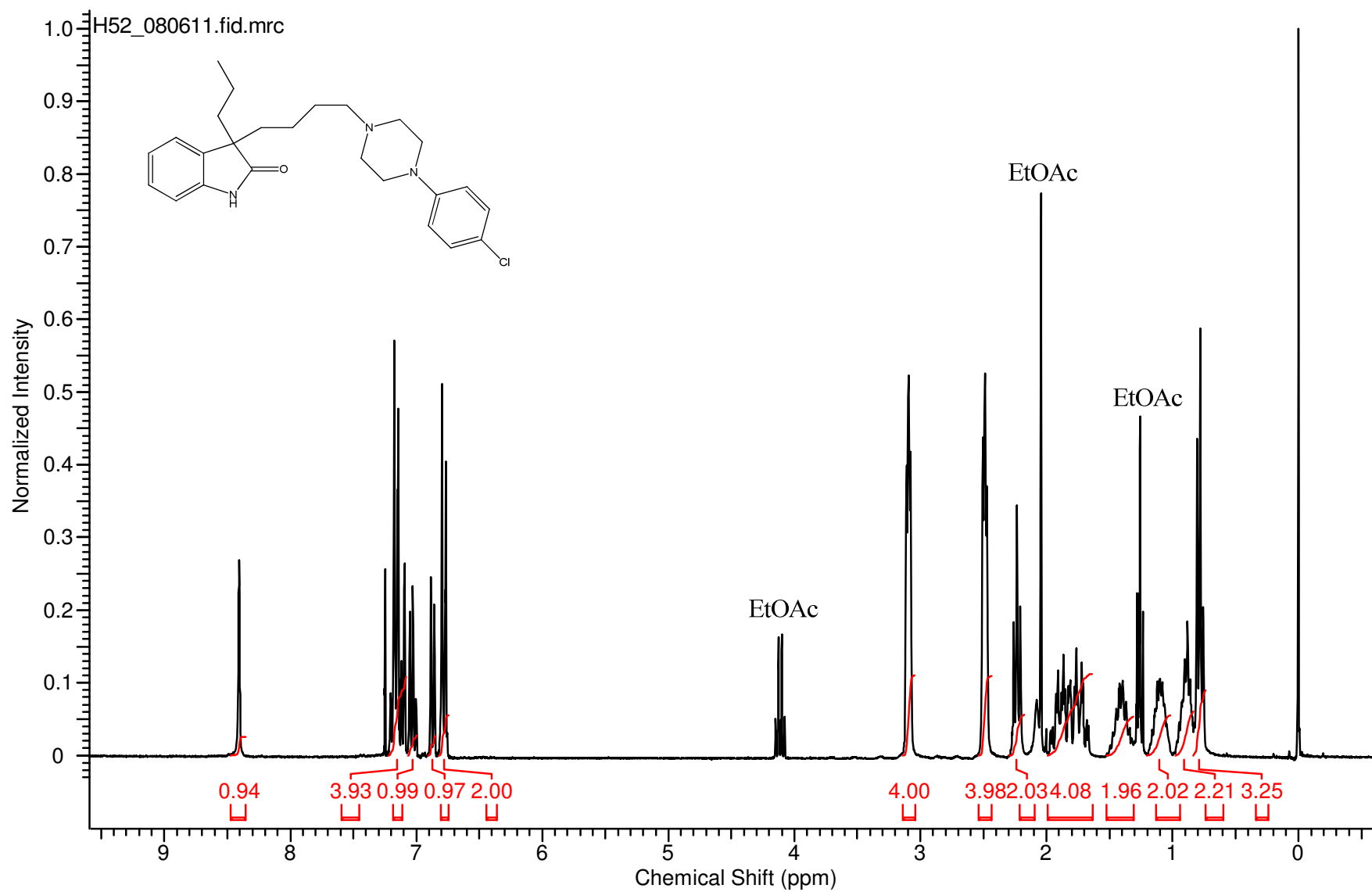


3-{4-[4-(4-Chlorophenyl)piperazin-1-yl]butyl}-3-methyl-1,3-dihydro-2*H*-indol-2-one (**17**)

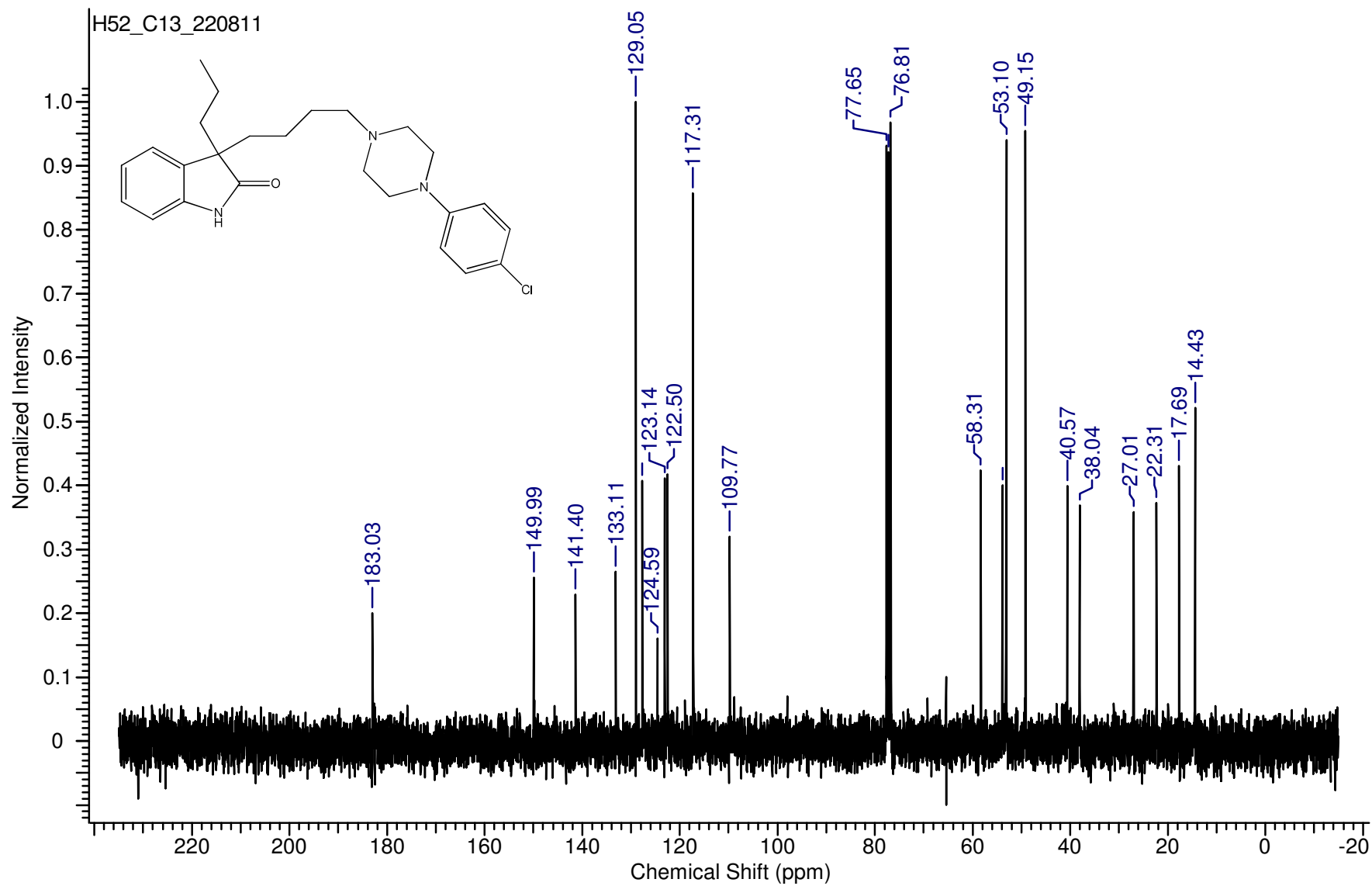
Spektrum:



3-{4-[4-(4-Chlorophenyl)piperazin-1-yl]butyl}-3-propyl-1,3-dihydro-2*H*-indol-2-one (**19**)

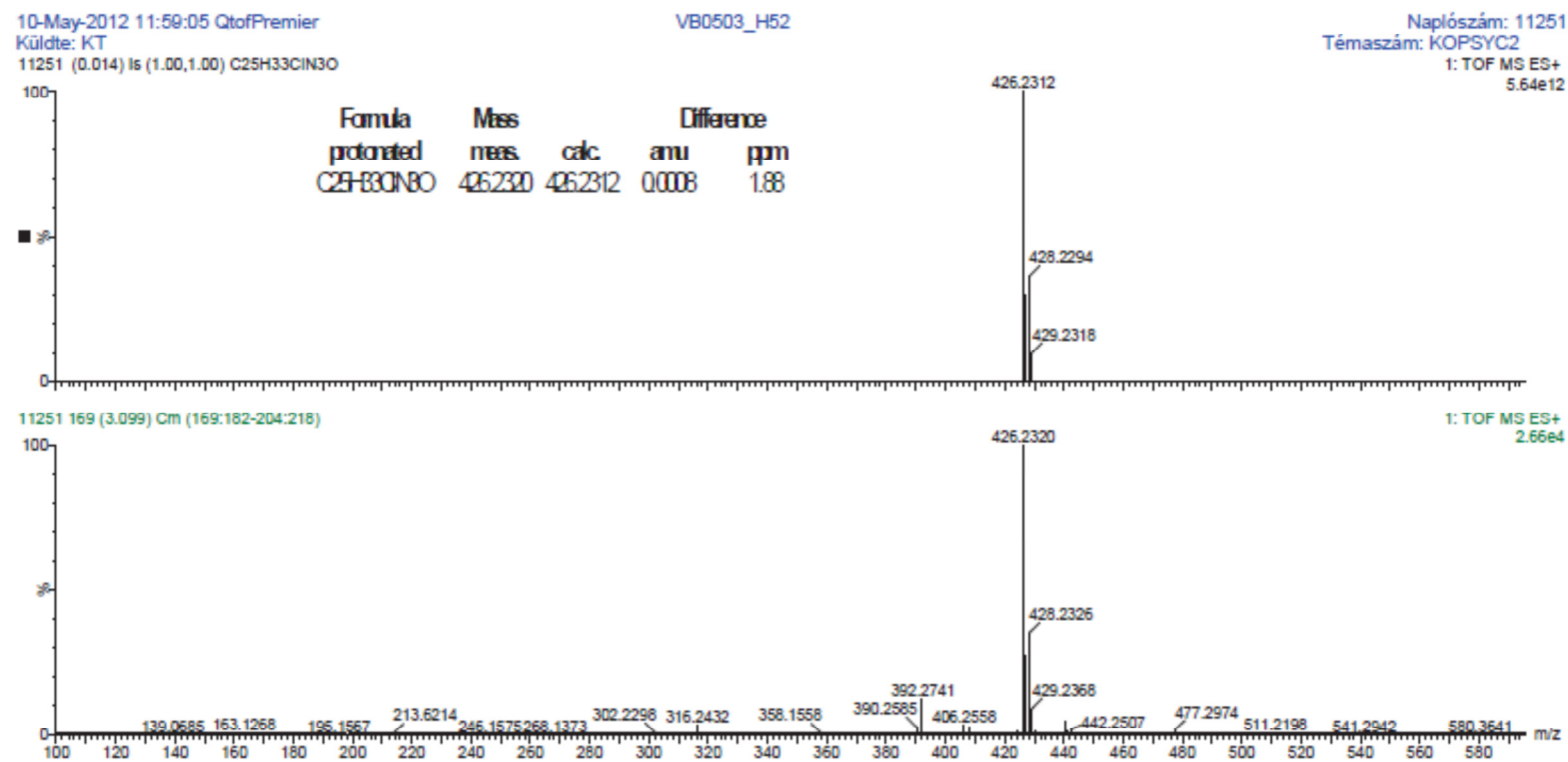


3-{4-[4-(4-Chlorophenyl)piperazin-1-yl]butyl}-3-propyl-1,3-dihydro-2*H*-indol-2-one (**19**)

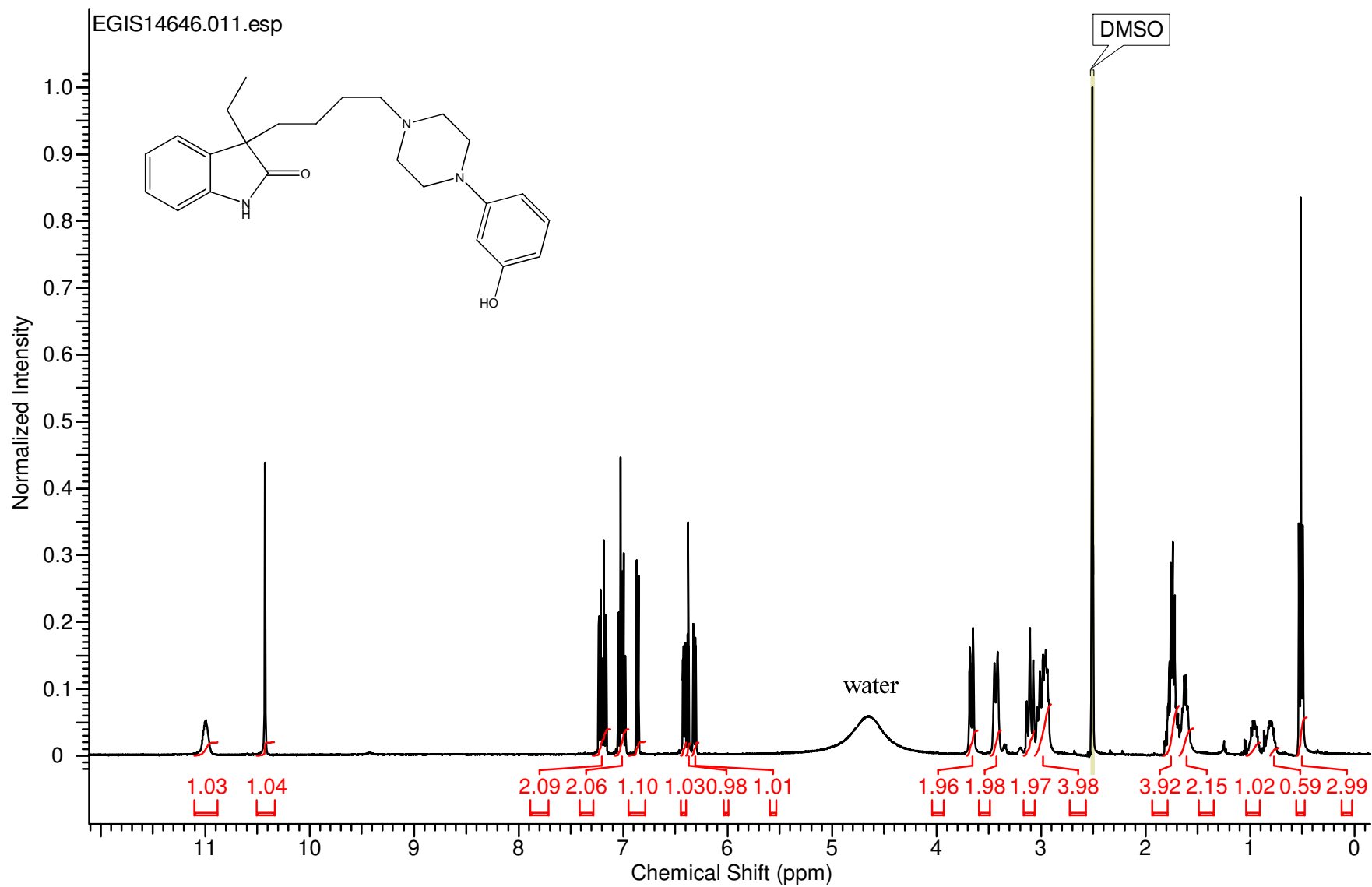


3-{4-[4-(4-Chlorophenyl)piperazin-1-yl]butyl}-3-propyl-1,3-dihydro-2*H*-indol-2-one (**19**)

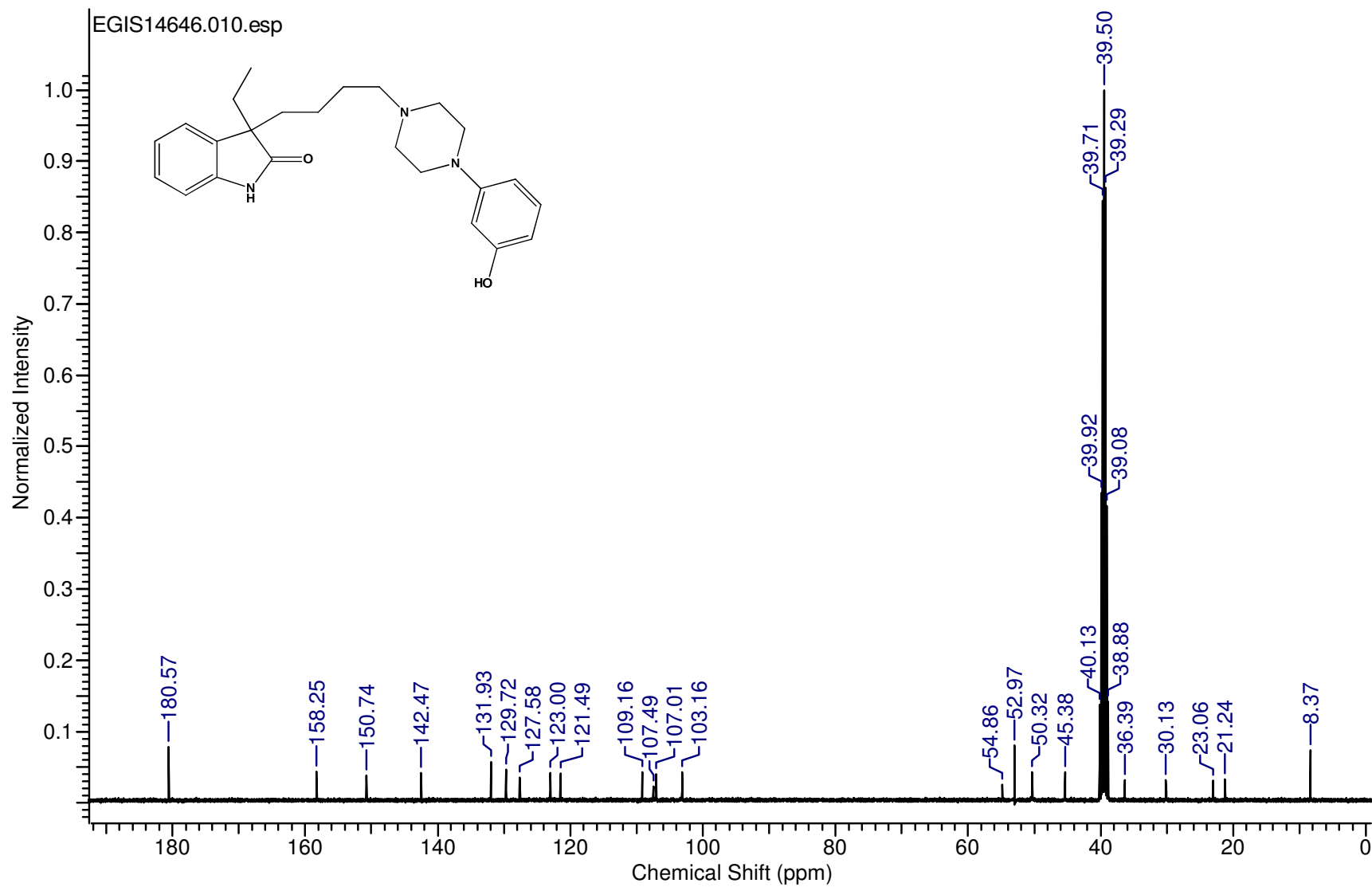
Spektrum:



3-Ethyl-3-{4-[4-(3-hydroxyphenyl)piperazin-1-yl]butyl}-1,3-dihydro-2H-indol-2-one (**10**)

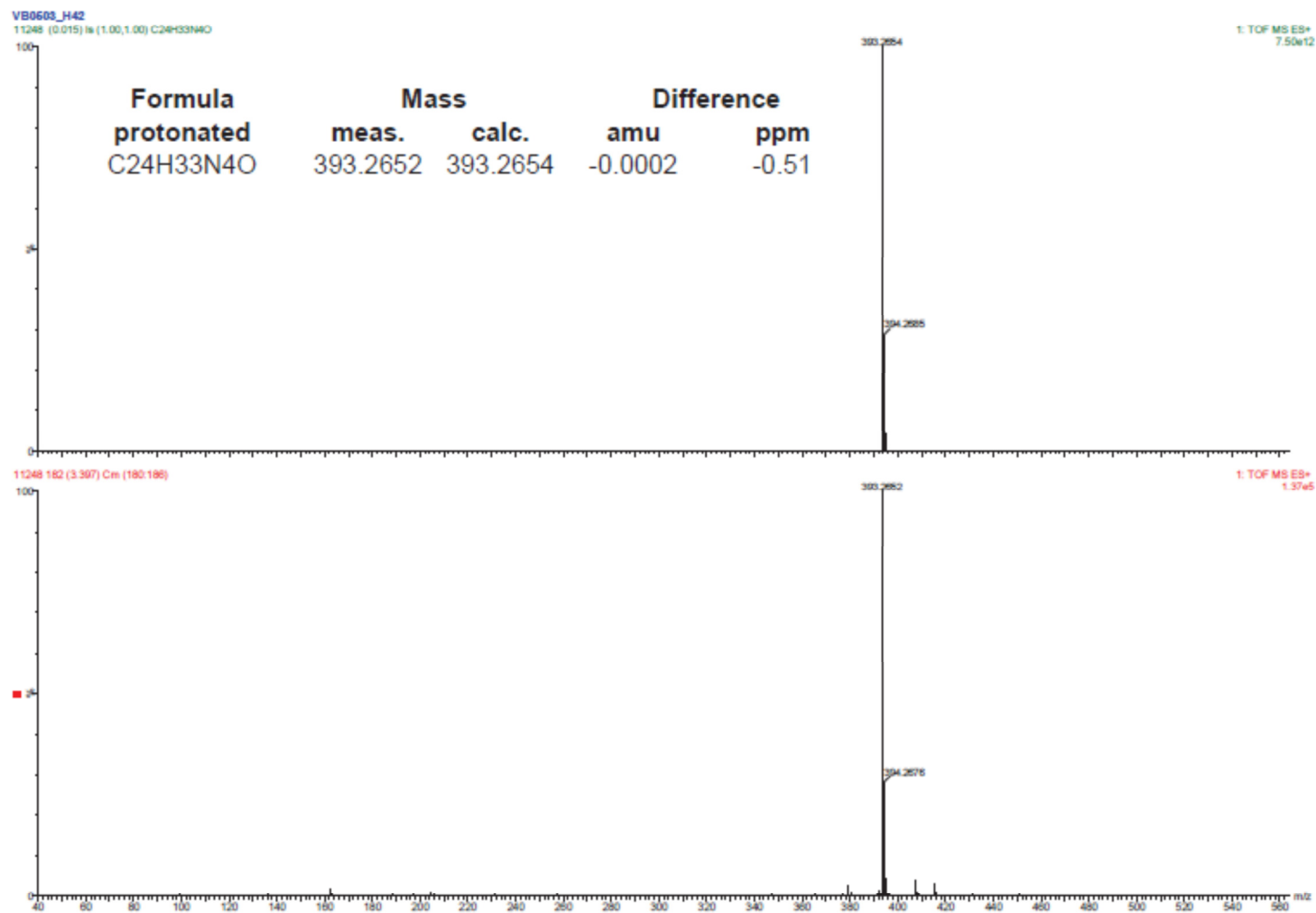


3-Ethyl-3-{4-[4-(3-hydroxyphenyl)piperazin-1-yl]butyl}-1,3-dihydro-2*H*-indol-2-one (**10**)

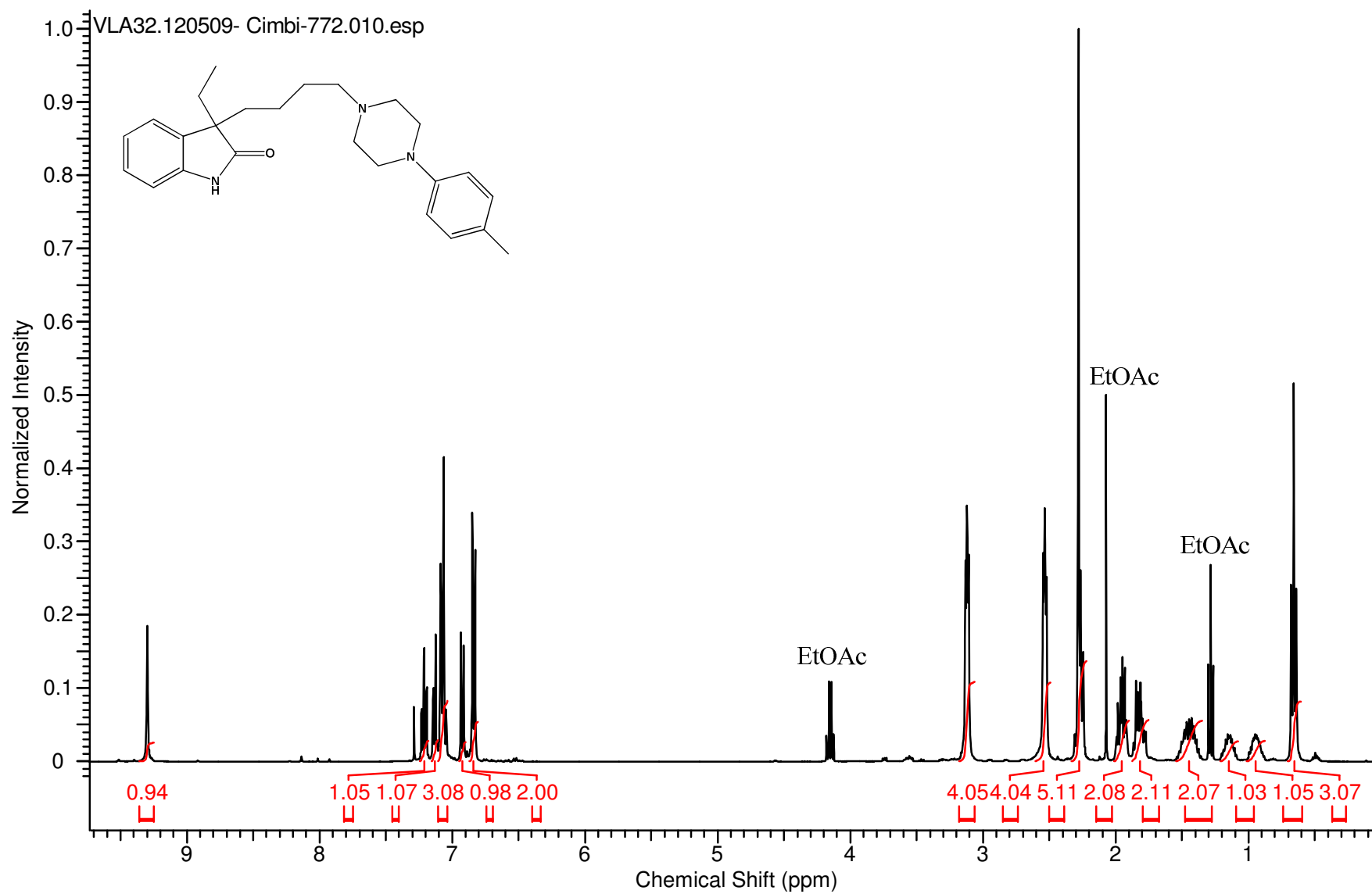


3-Ethyl-3-{4-[4-(3-hydroxyphenyl)piperazin-1-yl]butyl}-1,3-dihydro-2*H*-indol-2-one (**10**)

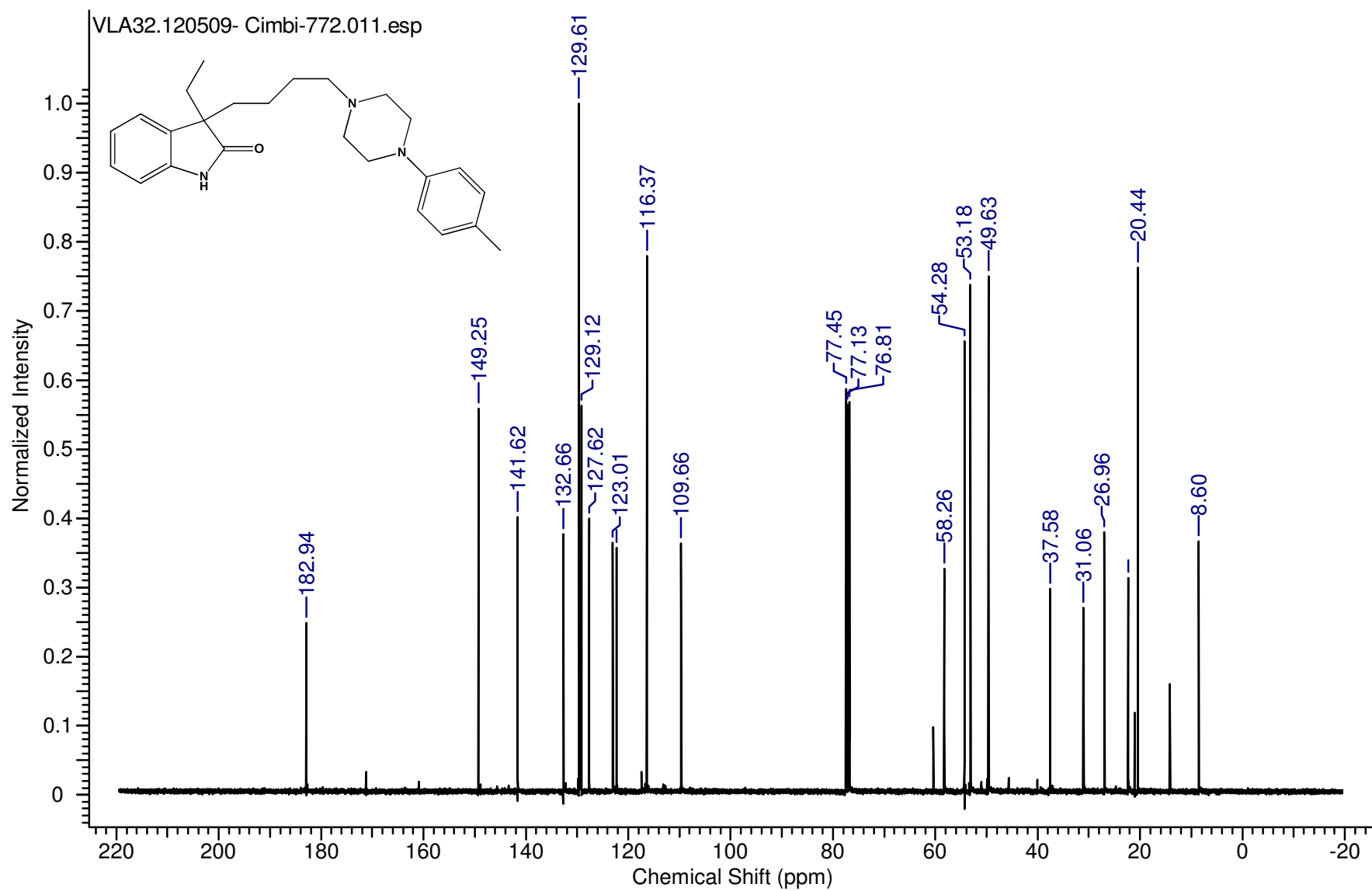
Spektrum:



3-Ethyl-3-{4-[4-(4-methylphenyl)piperazin-1-yl]butyl}-1,3-dihydro-2H-indol-2-one (**3**, Cimbi-772)

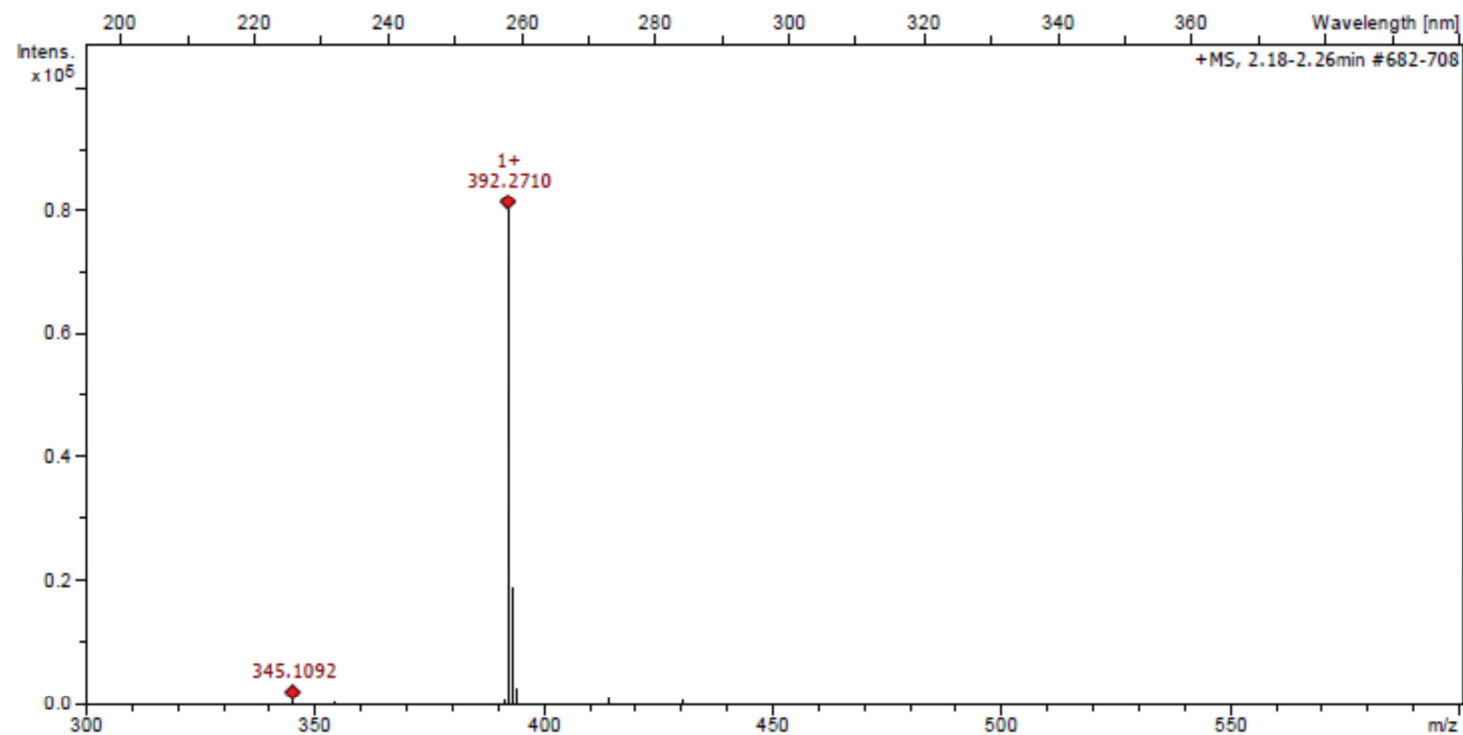


3-Ethyl-3-{4-[4-(4-methylphenyl)piperazin-1-yl]butyl}-1,3-dihydro-2*H*-indol-2-one (**3**, Cimbi-772)



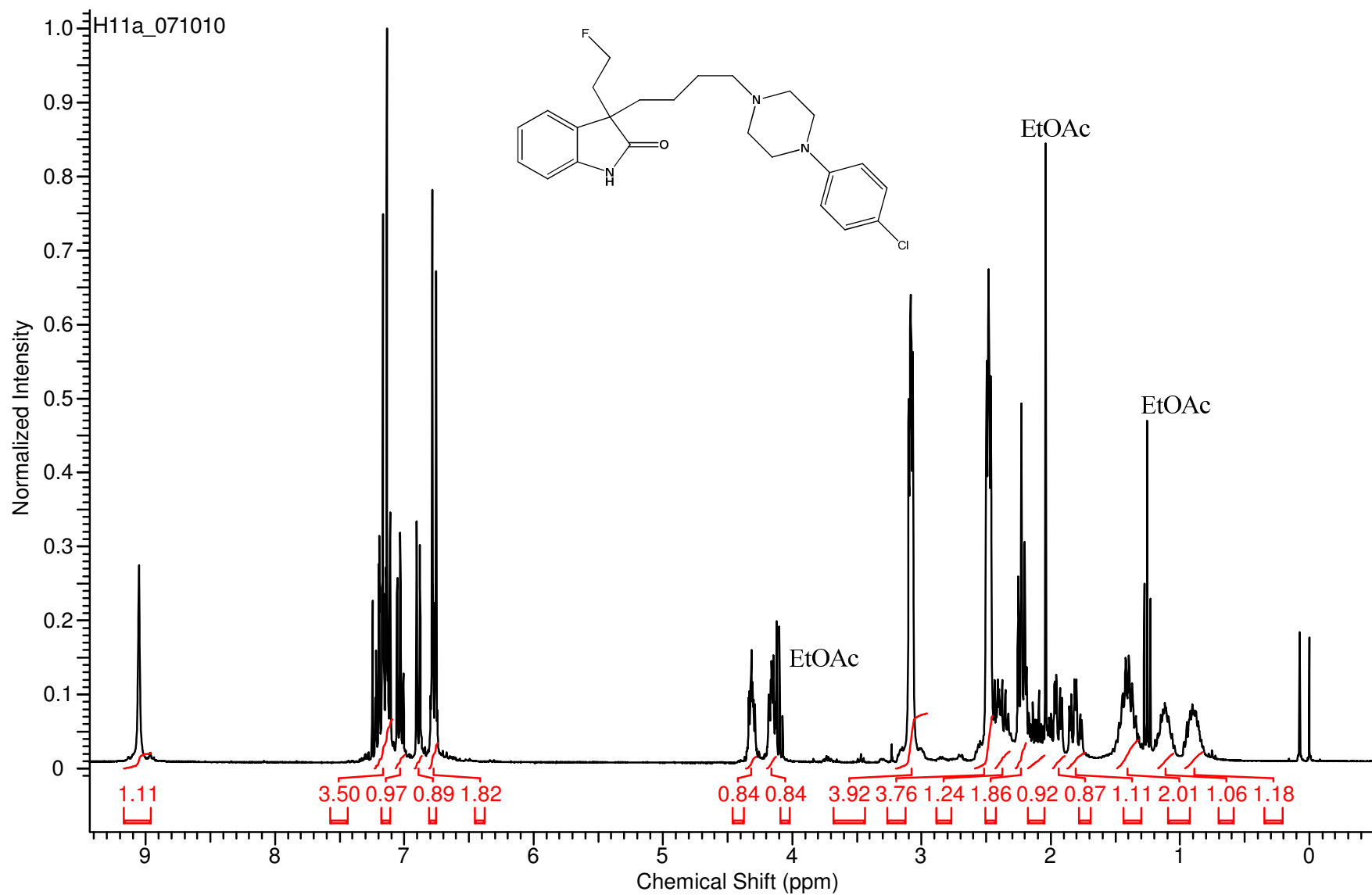
3-Ethyl-3-{4-[4-(4-methylphenyl)piperazin-1-yl]butyl}-1,3-dihydro-2*H*-indol-2-one (**3**, Cimbi-772)

Spektrum:

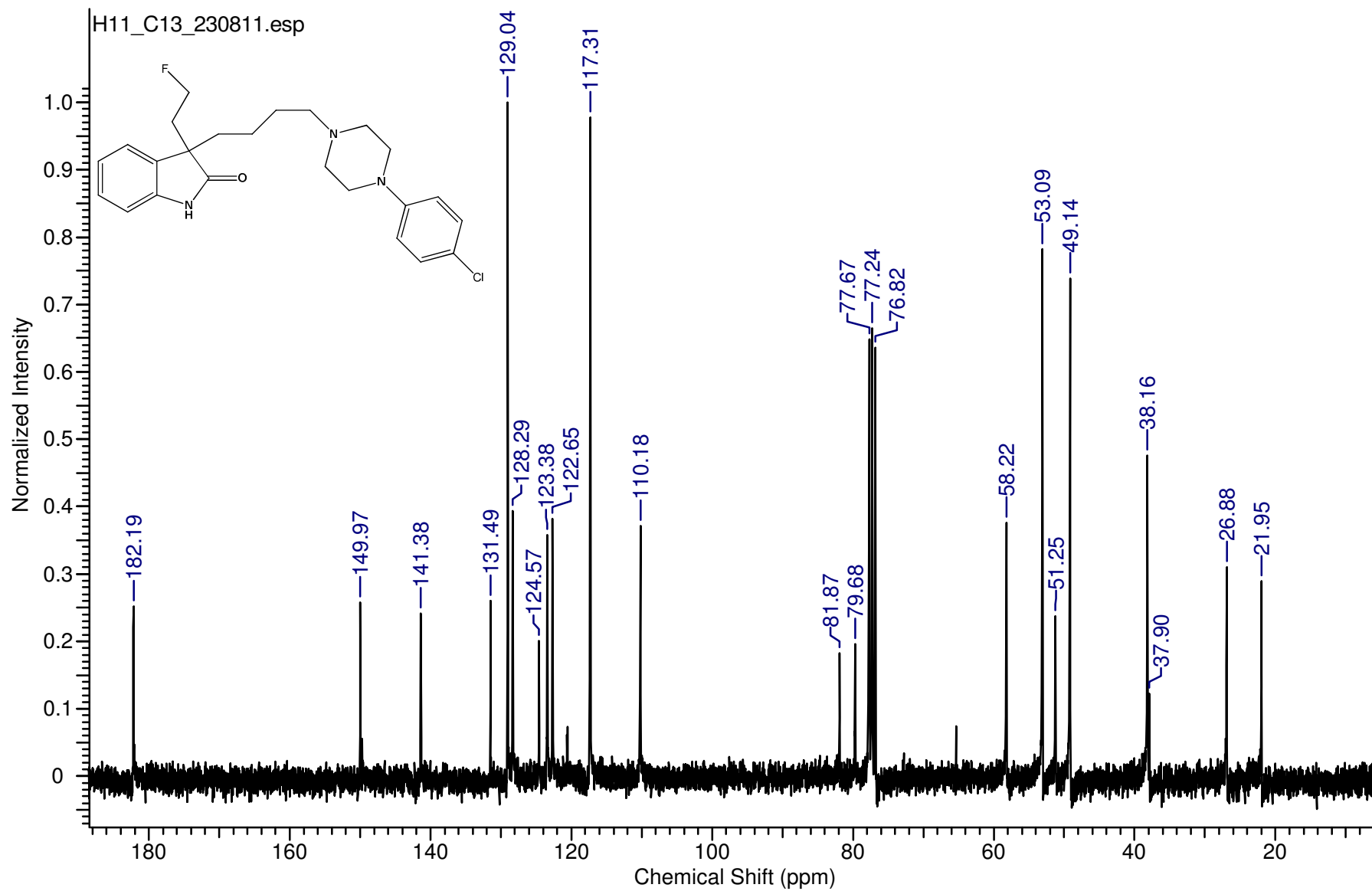


Meas. m/z	Ion Formula	Score	m/z	err [ppm]
392.271034	C ₂₅ H ₃₄ N ₃ O	100.00	392.269639	-3.6

3-{4-[4-(4-Chlorophenyl)piperazin-1-yl]butyl}-3-(2-fluoroethyl)-1,3-dihydro-2*H*-indol-2-one (**23**)

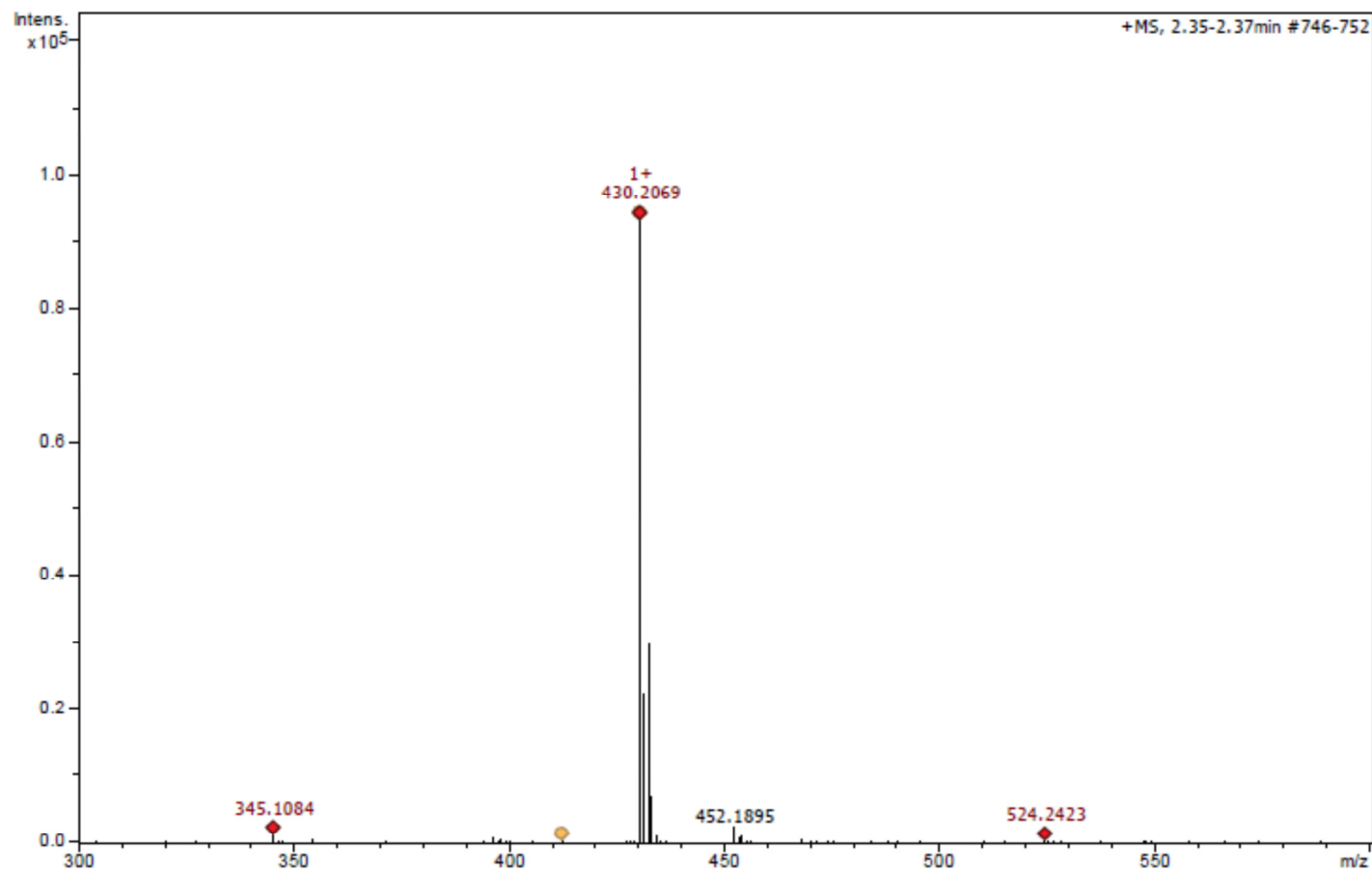


3-{4-[4-(4-Chlorophenyl)piperazin-1-yl]butyl}-3-(2-fluoroethyl)-1,3-dihydro-2*H*-indol-2-one (**23**)



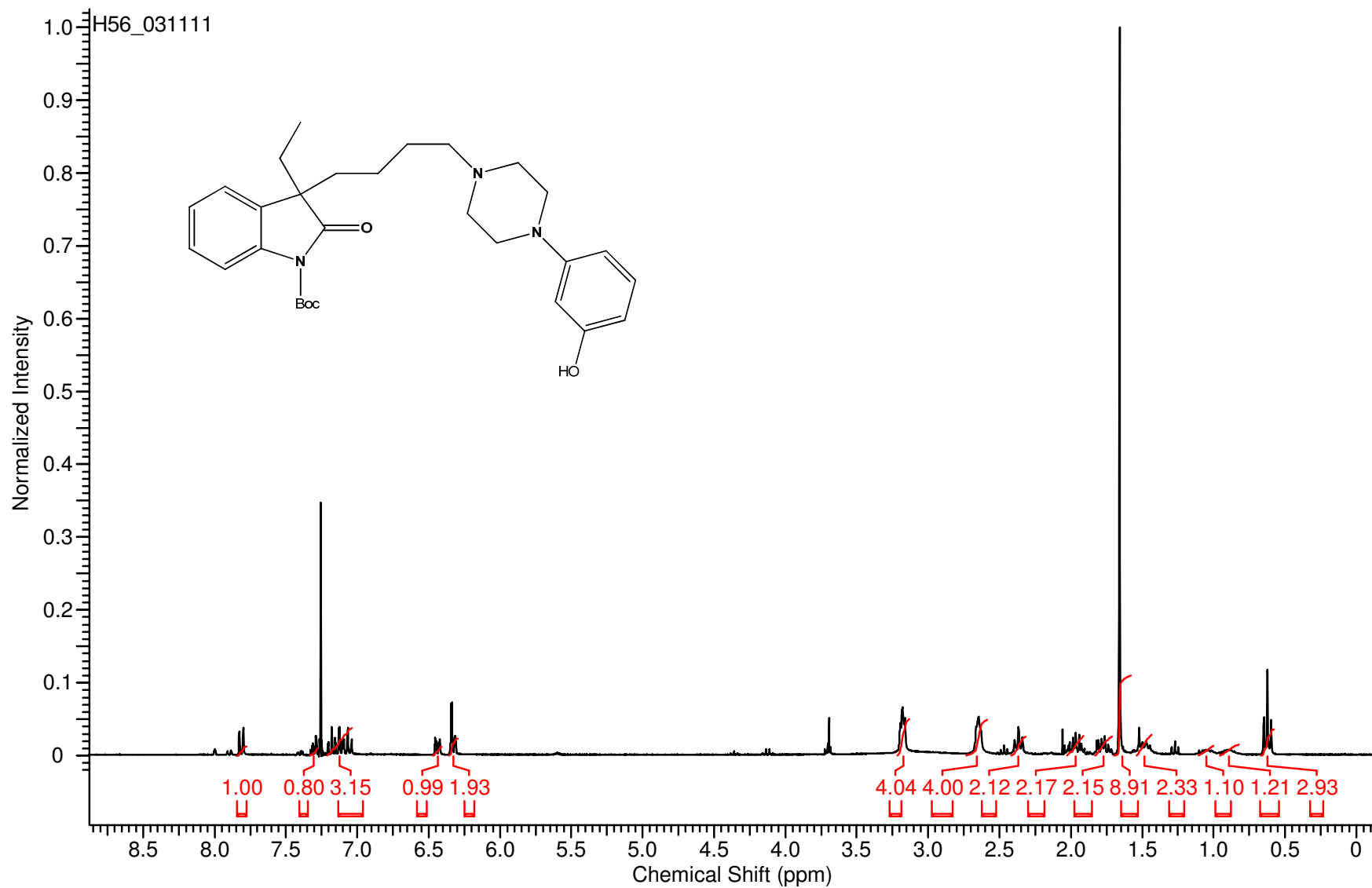
3-{4-[4-(4-Chlorophenyl)piperazin-1-yl]butyl}-3-(2-fluoroethyl)-1,3-dihydro-2*H*-indol-2-one (**23**)

Spektrum:

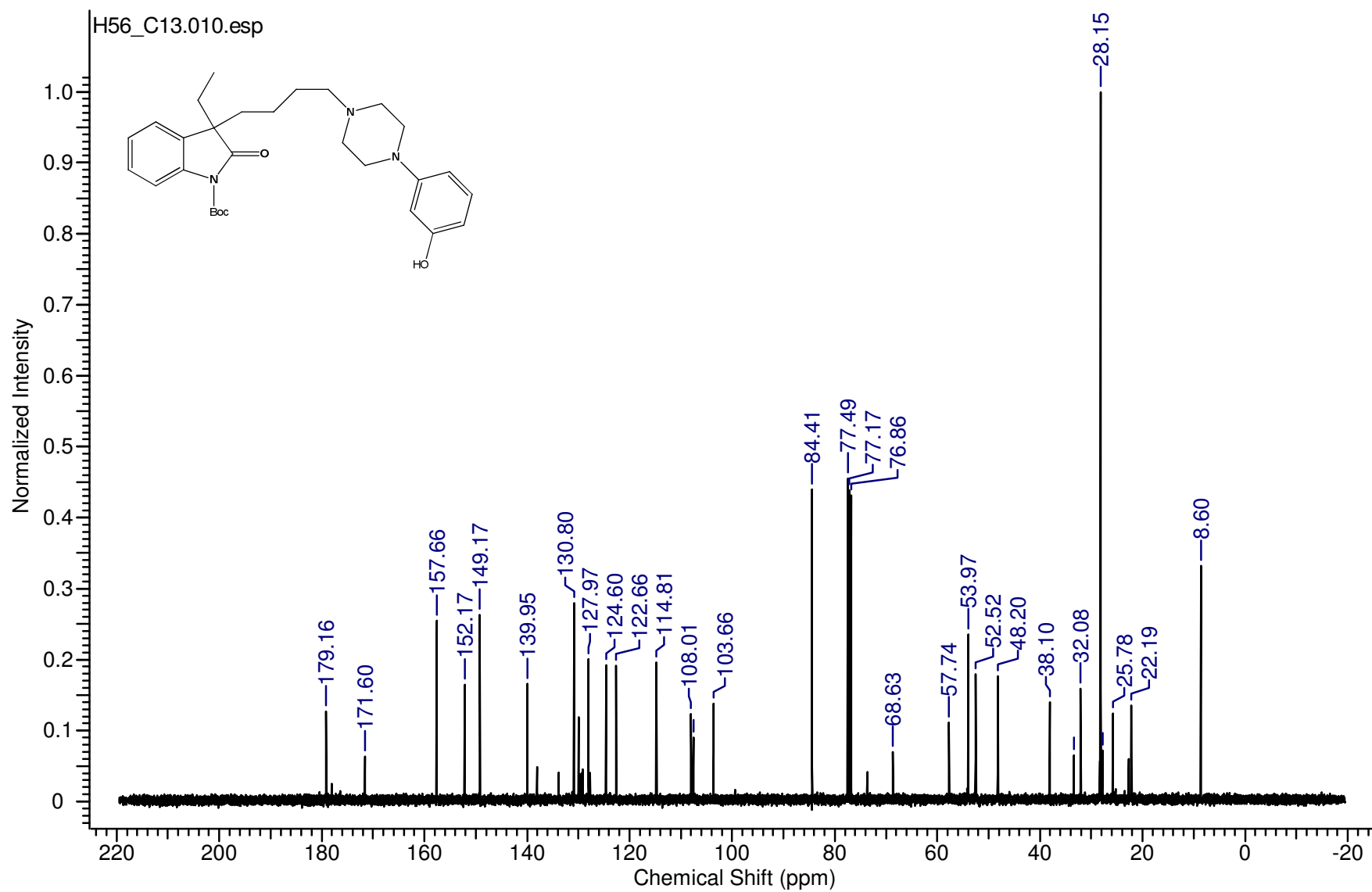


Meas. m/z	Ion Formula	Score	m/z	err [ppm]
430.206935	C ₂₄ H ₃₀ ClFN ₃ O	100.00	430.205595	-3.1

tert-Butyl 3-ethyl-3-{4-[4-(3-hydroxyphenyl)piperazin-1-yl]butyl}-2-oxo-2,3-dihydro-1*H*-indole-1-carboxylate (**11**)

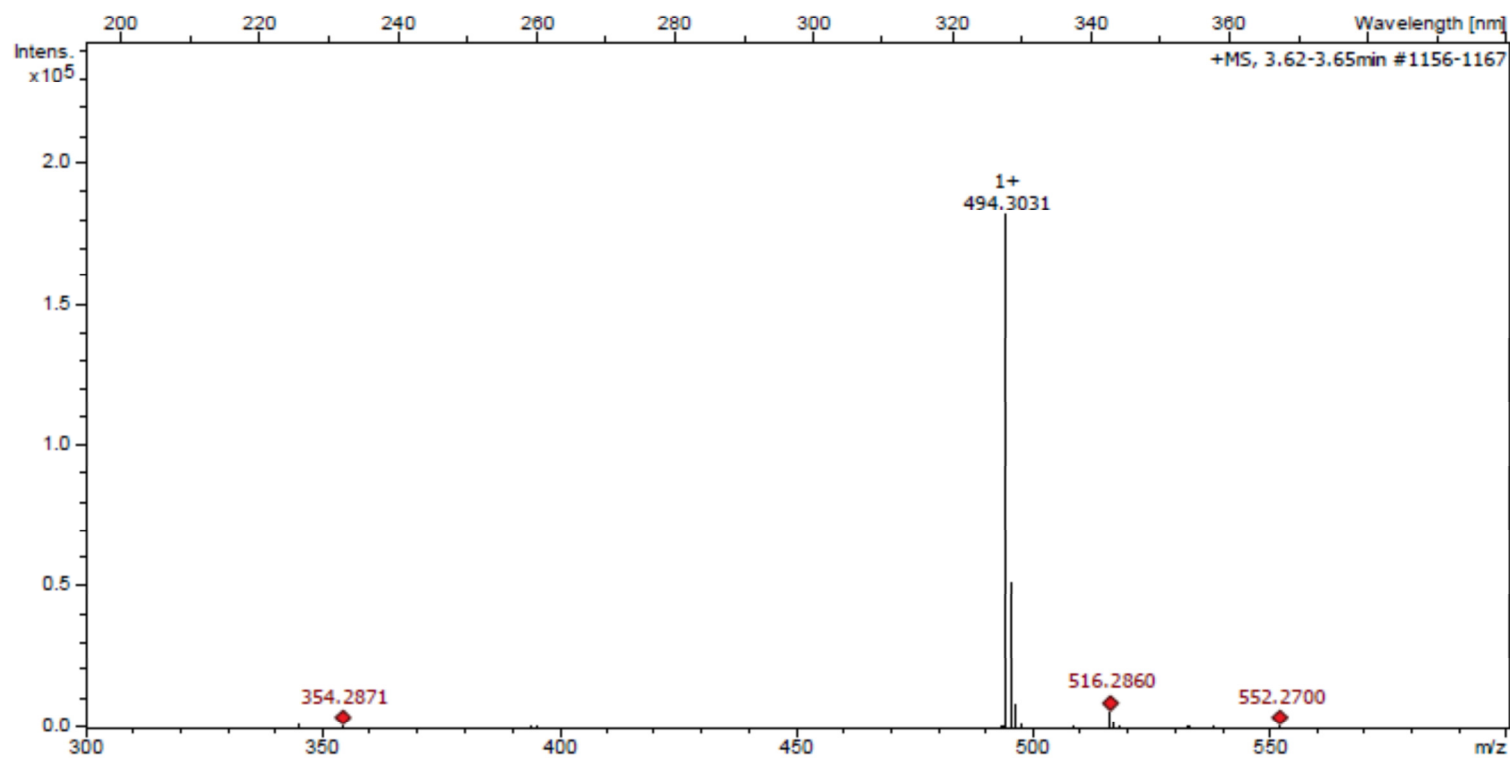


tert-Butyl 3-ethyl-3-{4-[4-(3-hydroxyphenyl)piperazin-1-yl]butyl}-2-oxo-2,3-dihydro-1*H*-indole-1-carboxylate (**11**)



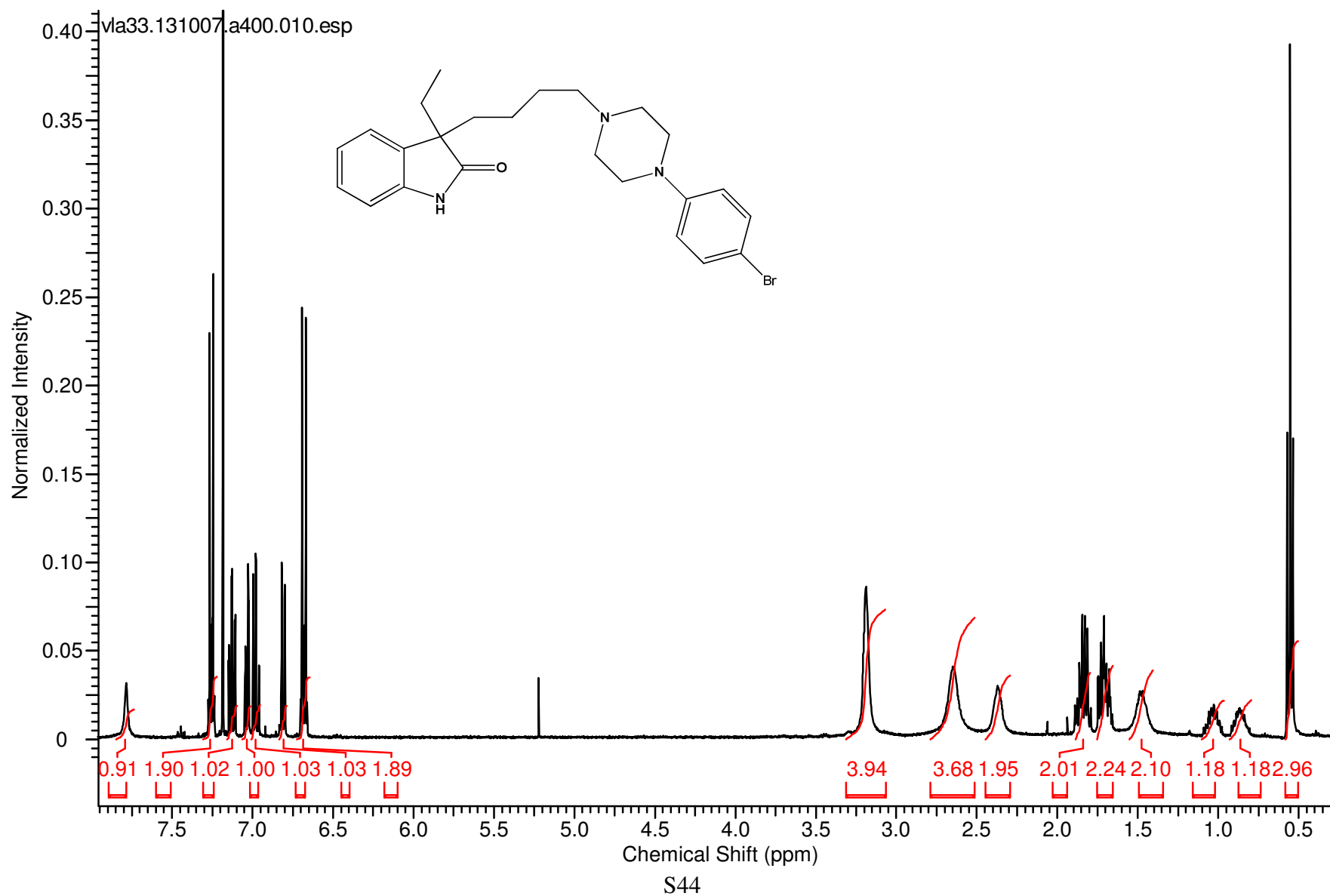
tert-Butyl 3-ethyl-3-{4-[4-(3-hydroxyphenyl)piperazin-1-yl]butyl}-2-oxo-2,3-dihydro-1*H*-indole-1-carboxylate (**11**)

Spektrum:



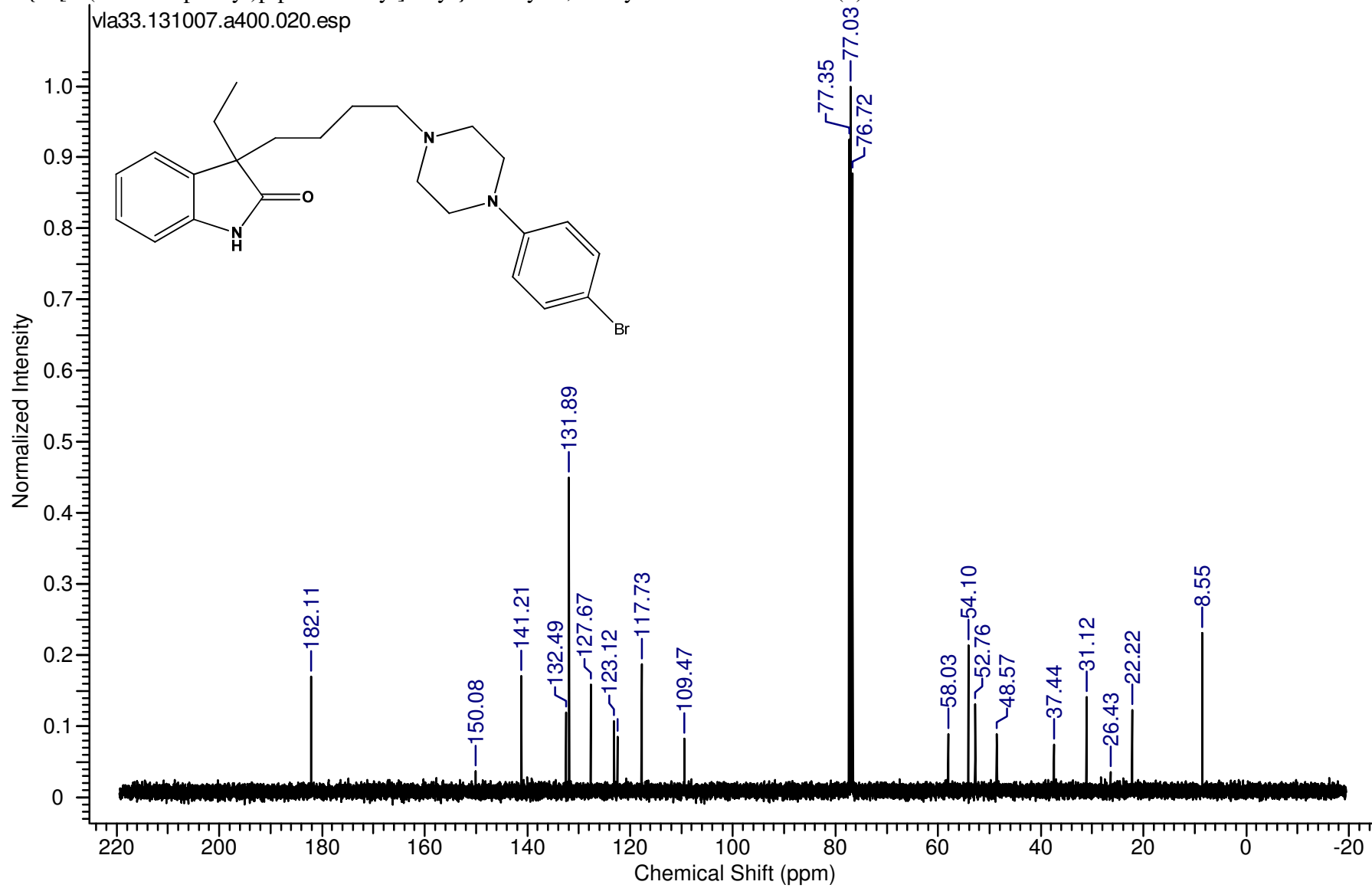
Meas. m/z	Ion Formula	Score	m/z	err [ppm]
494.303120	C ₂₉ H ₄₀ N ₃ O ₄	100.00	494.301333	-3.6

3-{4-[4-(4-Bromophenyl)piperazin-1-yl]butyl}-3-ethyl-1,3-dihydro-2*H*-indol-2-one (**7**)



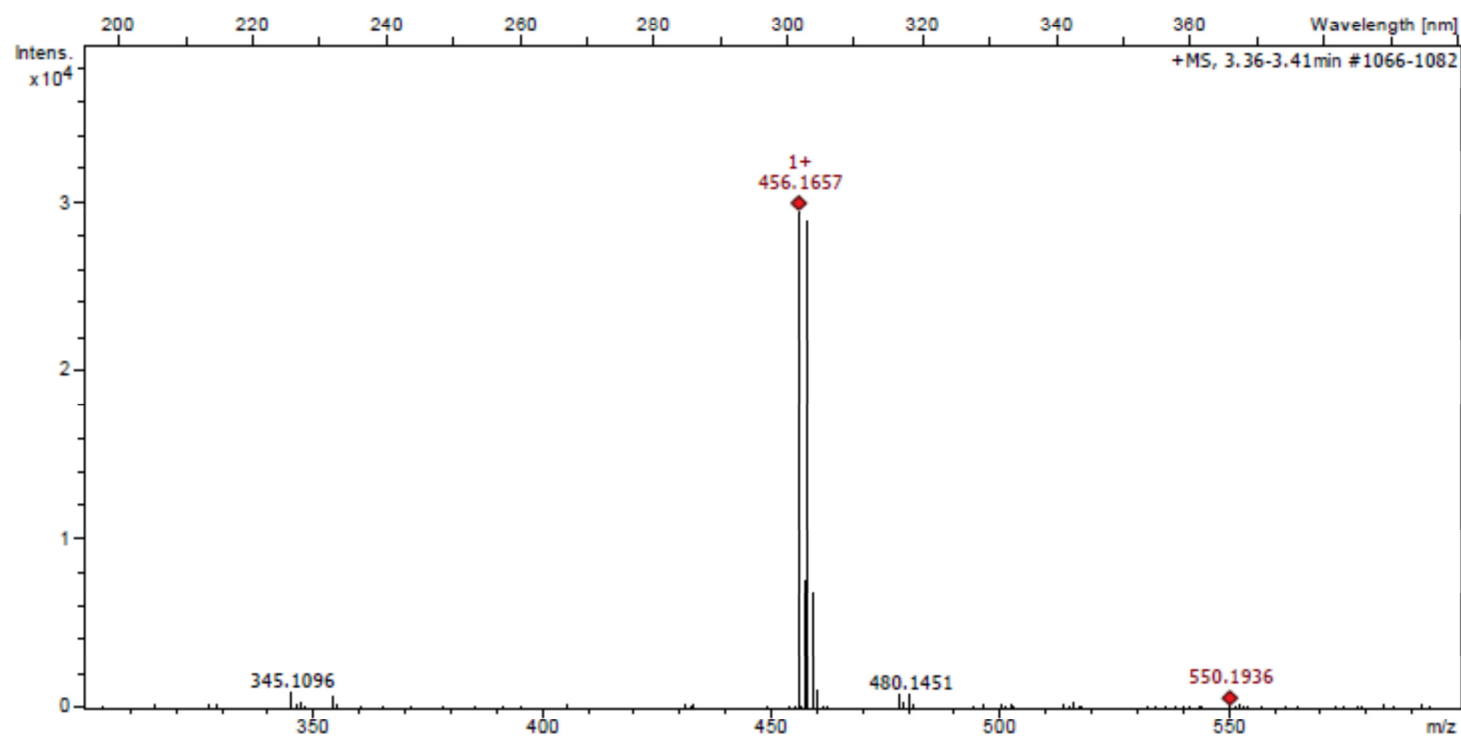
3-{4-[4-(4-Bromophenyl)piperazin-1-yl]butyl}-3-ethyl-1,3-dihydro-2*H*-indol-2-one (7)

vla33.131007.a400.020.esp



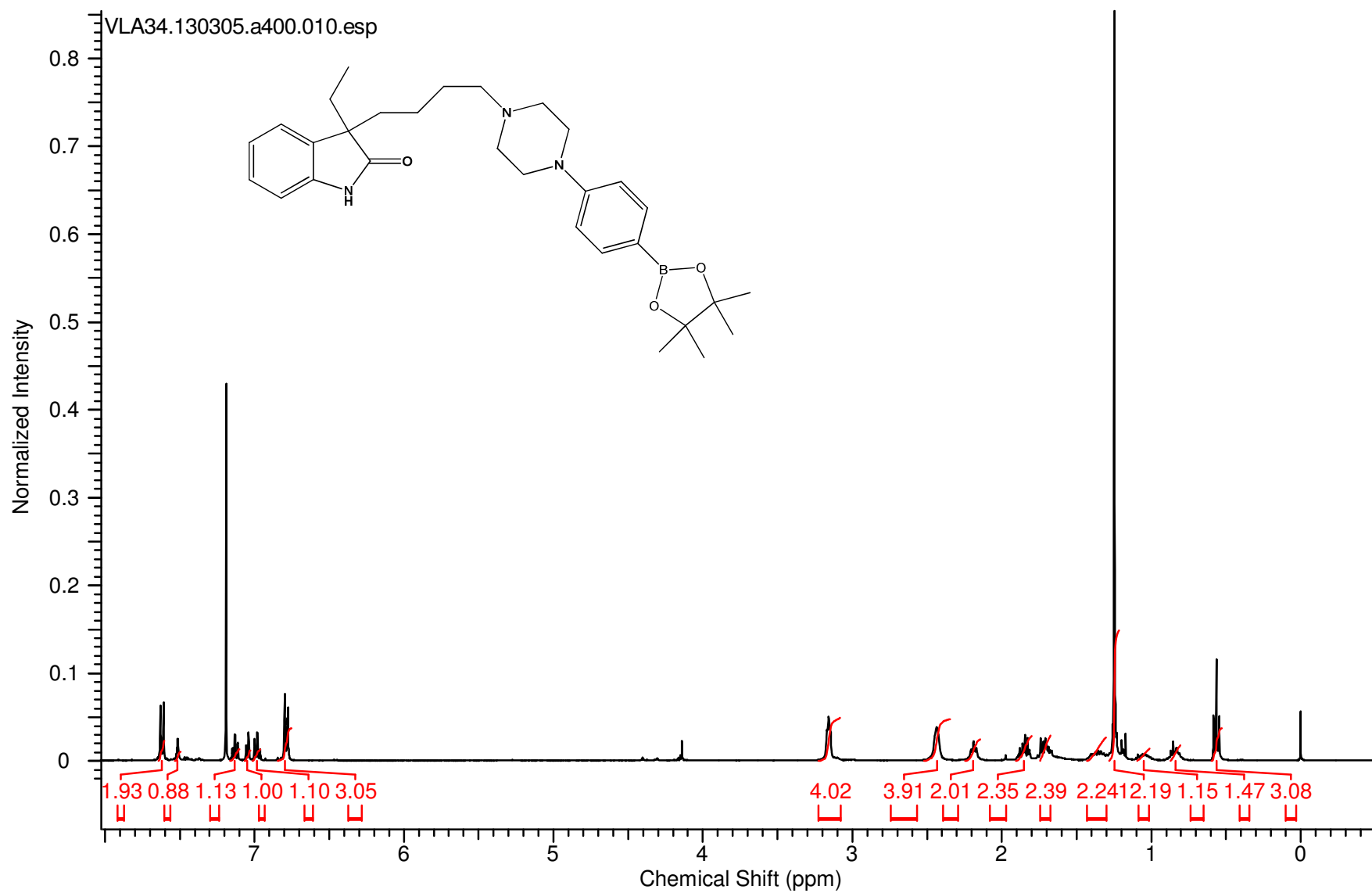
3-{4-[4-(4-Bromophenyl)piperazin-1-yl]butyl}-3-ethyl-1,3-dihydro-2*H*-indol-2-one (7)

Spektrum:

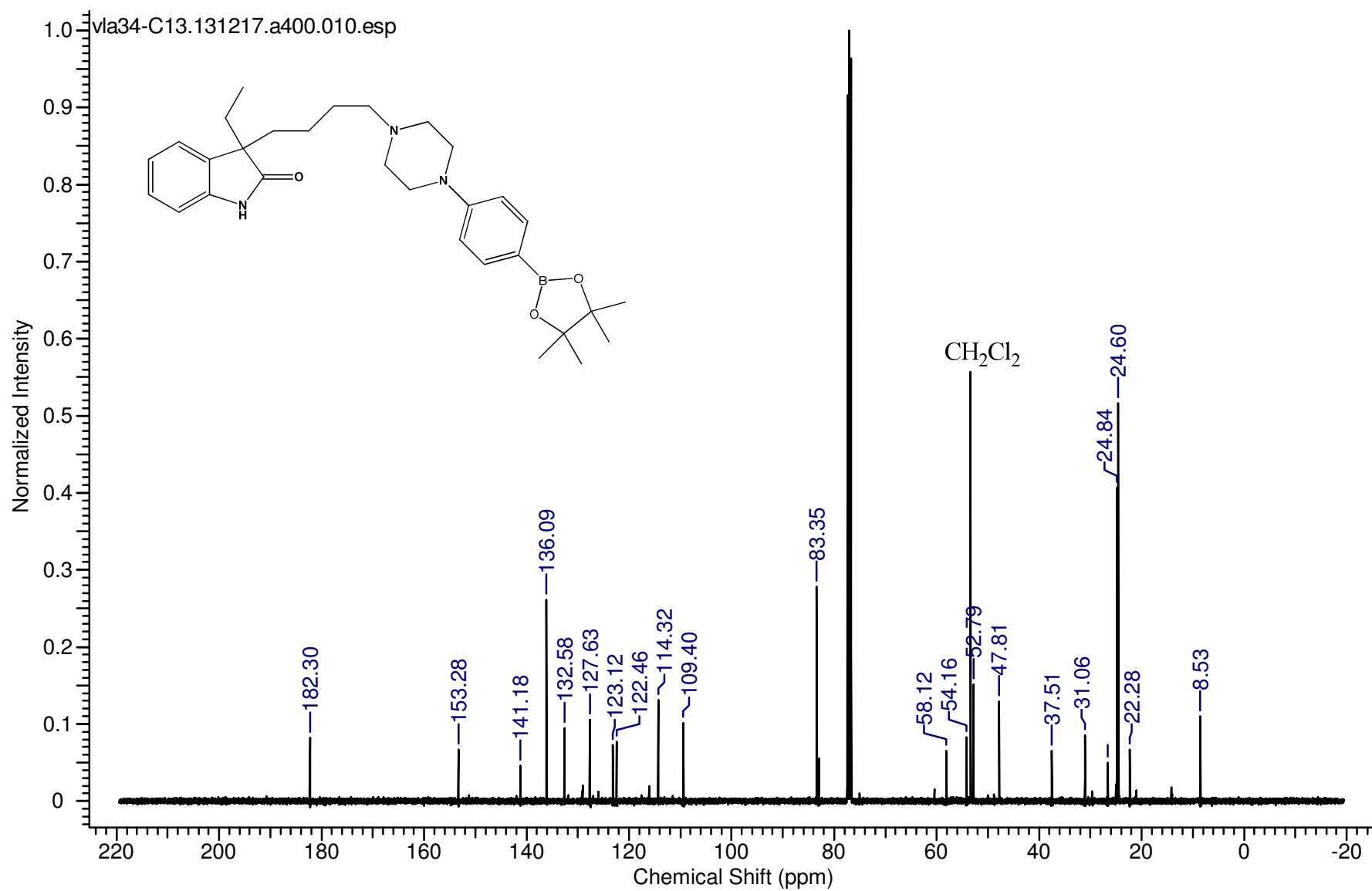


Meas. m/z	Ion Formula	Score	m/z	err [ppm]
456.165741	C ₂₄ H ₃₁ BrN ₃ O	100.00	456.164501	-2.7

3-Ethyl-3-(4-{4-[4-(4,4,5,5-tetramethyl-1,3,2-dioxaborolan-2-yl)phenyl]piperazin-1-yl}butyl)-1,3-dihydro-2H-indol-2-one (**8**)

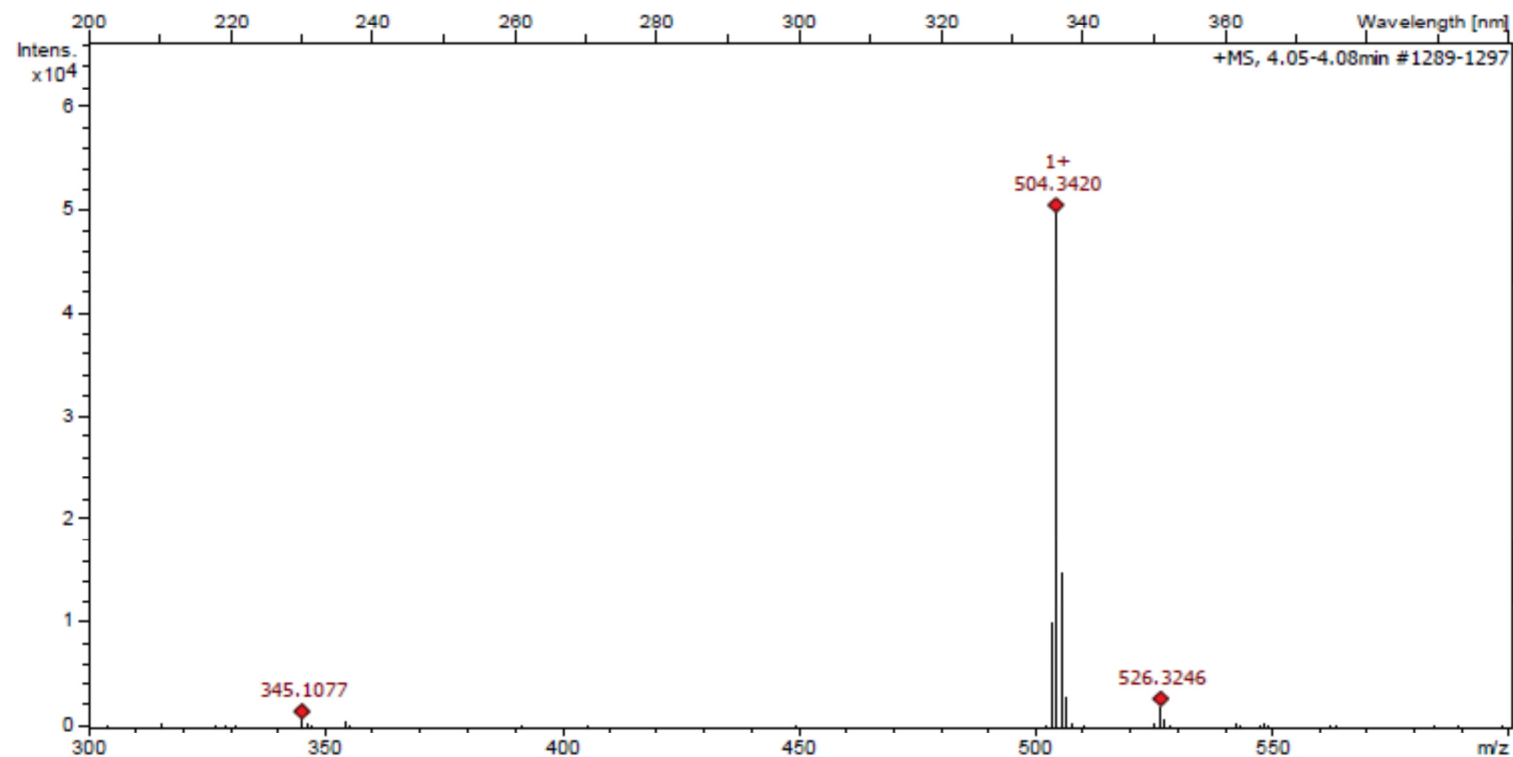


3-Ethyl-3-(4-{4-[4-(4,4,5,5-tetramethyl-1,3,2-dioxaborolan-2-yl)phenyl]piperazin-1-yl}butyl)-1,3-dihydro-2*H*-indol-2-one (**8**)



3-Ethyl-3-(4-{4-[4-(4,4,5,5-tetramethyl-1,3,2-dioxaborolan-2-yl)phenyl]piperazin-1-yl}butyl)-1,3-dihydro-2*H*-indol-2-one (**8**)

Spektrum:



Meas. m/z	Ion Formula	Score	m/z	err [ppm]
504.342027	C ₃₀ H ₄₃ BN ₃ O ₃	100.00	504.339733	-4.5